Colloidal interactions

REVIEW ARTICLE

Colloidal interactions

Luc Belloni

CEA/SACLAY, Service de Chimie Moléculaire, 91191-Gif-sur-Yvette Cedex, France

E-mail: `luc@scm.saclay.cea.fr`

Abstract. The present topical review describes the concept of effective interactions between spherical colloids in bulk solution. An introductive analysis based on the statistical mechanics of liquids and mixtures derives the main classes of colloidal forces observed at various solvent–solute compositions. A general survey of basic and advanced theories on ion-averaged interactions between charged colloids ends with a critical examination of recent statements on the existence of colloidal attraction and liquid–gas phase separation of pure electrostatic origin.

1. Introduction

As opposed to simple liquids, colloidal solutions are intrinsically complex systems containing *mesoscopic* particles, the colloids, in the nanometre to micrometre size range, and small solvent and solute molecules. The presence of solute components makes it possible to modify at will and on a large scale the static and dynamic macroscopic properties of the whole solution. Many organic/inorganic, natural, industrial and biological systems correspond to this schematic picture. Micelles, mineral oxide particles, polymer latices, soluble proteins, clay platelets, surfactant lamellae etc represent the colloid component. The stability of the solution with respect to irreversible coagulation or reversible aggregation and phase transition as well as its rheology are controlled by the addition of ions (in polar solvents), complexing molecules, adsorbing or non-adsorbing polymers, ... Due to the large asymmetry in size, mass and time scale between the colloidal particles and solvent/solute molecules, most of the experimental techniques are directly sensitive only to the former. Examples are light and small angle x-ray or neutron scattering and direct optical visualization. It is thus tempting to forget, at least explicitly, about the small species and to consider the colloidal solution not as a mixture but as a monodisperse system formally equivalent to a simple liquid, the colloids playing the role of atoms. The central question in this one-component picture is the determination of the effective interaction potential or force between colloids which implicitly accounts for the solvent effects. The denomination 'colloidal interactions' refers to this indirect, solvent-averaged quantity.

Any standard theory of simple liquids first assumes a basic, unambiguous form for the potential of interaction between atoms or molecules (hard-core short range repulsion, charge–charge and multipolar coulombic contribution, . . .), then solves the N-body statistical mechanics problem. In this case, the central question is: for a given pair potential $v(r)$ (energy of interaction of an isolated pair in vacuum as a function of the separation r), what is the pair distribution function $g(r)$ (normalized probability to find a pair in the configuration r inside the concentrated liquid) from which most of the equilibrium and structural properties can be directly derived [1]? The situation in colloidal systems is somewhat reversed: one must first

perform complex statistical averages, this time over the degrees of freedom of the solvent (including solute) molecules, before deriving the effective colloidal interactions. When an isolated spherical particle is immersed in the bulk, the solvent structure is locally perturbed around it, up to a distance λ from its surface. When two such particles approach each other, the modified solvent 'shells' begin to overlap and the local fluid structure becomes highly directional. It is this spherical imbalance which results in an effective force F acting on the colloids. The nature, the strength and even the sign of F are not obvious and depend on the details of the solvent–solvent and solvent–colloid direct interactions. Assuming that colloids in solution only interact by pairs, the effective or mean force pair potential $v^{eff}(r)$, from which F is derived, then becomes the starting point in the standard, one-component calculation of the colloidal correlations. This intermediate function $v^{eff}(r)$ is the key in the powerful concept of colloidal interaction. Depending on the domain of interest, one focuses on either the first or the second step in the averaging process. In the former case, the potential is carefully determined as a function of solvent/solute composition and colloid nature and dimension. (For large colloids of radius $R \gg \lambda$, the interaction takes place only near contact. In that regime of surface to surface separation $h \ll R$, the surface curvature has a trivial effect: according to the Derjaguin approximation, F/R is independent of R and can be expressed as πE, where E is the interaction energy per unit area between two parallel, infinite, flat colloidal surfaces separated by the distance h. Thus, most of the theories are developed in this simpler planar geometry. For smaller colloids, the finite curvature must be taken explicitly into account.) In the latter case, the richness of form in $v^{eff}(r)$ induces a wide spectrum of structural and phase behaviour in concentrated colloidal fluids, much wider than in simple liquids.

The situation becomes quite complicated if the colloids interact not only by pairs but also by triplets, ... This happens when the solvent shell thickness λ is not negligible compared to the dimension R and the mean distance between first colloid neighbours, as in highly deionized charge-stabilized colloidal solutions (λ representing the Debye length). The overlap of the spheres of interaction (radius $\approx R + \lambda$) and the resulting colloidal interaction have a multiple-body character and cannot be decomposed as a sum of pair contributions as before. The N-body potential of mean force depends on the relative positions of all colloids inside the solution. Although of formal interest, its practical use for illustrating the solvent effect and calculating the colloid correlations is less trivial than in the pair-wise additive situation.

The experimental techniques used to determine colloidal interaction forces/potentials fall in two complementary categories. For submicronic particles, the direct measurement of pair interactions of two isolated colloids is not possible due to technical limitations in visualization, separation control and force evaluation. On the other hand, the use of the thermodynamic balance against the thermal energy kT ($\approx 4 \times 10^{-21}$ J at room temperature) and statistical averages over $N \approx 10^{23}$ particles induce macroscopic behaviours from which interaction curves can be indirectly extracted. The scattered intensity $I(q)$ as a function of the scattering vector q and the osmotic pressure Π are widely used quantities which allow quantitative evaluations. Light and small angle x-ray and neutron scattering offer a q-range of 10^{-4}–1 Å^{-1} which is ideally suited for the study of submicronic colloidal systems [2]. Due to obvious experimental limitations (finite number of points in a restricted domain of scattering angle, non-perfect precision of the data etc), the usual procedure consists of the following steps: (i) assume pair-wise additivity for the colloidal interactions, (ii) start *a priori* with a simple form for the effective potential $v^{eff}(r)$ including a few parameters (size, effective charge, adhesiveness, ...), (iii) solve accurately if not exactly the N-body problem of statistical mechanics and (iv) compare the result with experimental spectra and adjust the parameters to reach a reasonable agreement [3]. Concerning the osmotic pressure, the combination of various

techniques covers the broad range 10^{-4}–10^{+9} Pa. Differences of absolute pressures between solution and solvent reservoir through a membrane ($\Pi = 1$–10^6 Pa), solvent vapour pressures above the solution (10^5–10^9 Pa) are measured directly or indirectly by equilibration with a previously calibrated reference system [4–6]. Analysis of a single sedimentation (10^{-4}–1 Pa) [7] or centrifugation (10^5–10^7 Pa) [8] profile for heavy enough colloids also makes it possible to determine the equation of state of the solution for a wide range of concentrations/pressures. The theoretical interpretation of Π in terms of colloidal interactions requires the same statistical treatment as before. A notable exception concerns lamellar systems where the osmotic pressure is identified with the pair force per unit area ($\equiv -\,\mathrm{d}E/\mathrm{d}h$) between infinite parallel plates.

The second category of experiments measures directly the force law between large enough particles. With the surface force apparatus (SFA) [9] and atomic force microscope (AFM) [10], two macroscopic curved surfaces (mean radius of curvature R) immersed in a liquid are brought towards each other in a highly controlled way using piezoelectric crystals; the separation distance h is measured through optical devices in the range 0–100 nm with a precision of 1 Å; the force F is deduced from the deviation of cantilever springs of calibrated spring constant. The ratio F/R is obtained in the range 10^{-6}–10^{-2} N m^{-1}. According to the Derjaguin approximation, the resulting force law $F/R(h)$ can be identified with the corresponding law for large colloids immersed in a solution, at constant geometry, material and solvent composition.

Modern techniques have been recently developed for direct measurement of colloidal pair interactions in bulk. In paramagnetic oil droplet suspensions, the formation of aligned chains of particles is observed under an applied magnetic field [11]. At equilibrium, the unknown colloidal repulsion between two successive colloids is exactly balanced by a dipolar magnetic attraction of known strength while the separation is measured through light diffraction. With the total internal reflection microscopy (TIRM) [12], the fluctuating position of a colloidal sphere ($R \geqslant 1~\mu$m), subject to gravity, located above a glass plate, is analysed in terms of the wall–sphere potential law. In other methods, video microscopy allows a direct observation of colloidal configurations in bulk [13, 14] or near walls [15, 16]. The potential of interaction is extracted from the measured pair distribution function [13, 15]. A related technique catches with optical tweezers isolated pairs of colloidal particles [14, 16]. After release of the external constraint, the relative Brownian motion of the interacting particles is followed.

The main purpose of the present topical review is to convince non-specialists that the variety of effective colloidal interactions can be understood in a systematic and quantitative way using a simple albeit accurate description of the solvent/colloid correlations. The modern general formalism of statistical mechanics of liquids and asymmetrical mixtures is recalled in section 2 with a careful presentation of the notions of N-body potential of mean-force and effective pair potential in the concentrated regime. Although most of the concepts are valid for different geometries, the focus is on solutions of *spherical* particles. The specific properties of elongated, rodlike or flexible colloidal systems are not addressed. Section 3 reviews the different classes of effective interaction between pairs of colloids expected in neutral systems as a function of solvent–solvent and colloid–solvent affinities. Section 4 deals with electrostatic interactions between charged colloids in concentrated solution. The general survey includes advanced as well as basic, Debye–Hückel-like, theories. This somewhat lengthy presentation leads to a critical examination of recent statements in the literature and clarifies the important notion of ion-averaged attraction and liquid–gas phase separation of pure electrostatic origin. Finally, section 5 evokes briefly the fundamental van der Waals force as well as the miscellaneous interactions which result from complex couplings between electrostatic, van der Waals and discrete solvent effects.

2. Direct, mean force, effective potentials of interaction

The purpose of the present formalism is to transform solvent–colloid mixtures into colloidal 'gases'. What are the effective, solvent-averaged interactions? To what extent do the text-book concepts and formula of simple liquids [1], briefly recalled in 2.1, remain valid in the effective, one-component approach?

2.1. Monodisperse systems

We consider N spherical particles in a volume V at the temperature T interacting via the pairwise additive potential $U_N(r^N) = \sum_{i<j} v(r_{ij})$. $v(r)$ represents the direct pair potential between two isolated particles in vacuum and is, in principle, independent of T and of the density $\rho = N/V$. The direct, pair force is $f(r) = -v'(r)$. Examples of $v(r)$ are the hard-sphere, soft-sphere, Lennard-Jones, square-well, ... potentials.

In the canonical ensemble, the pair distribution function $g(r)$ is given by

$$g(r_{12}) = \frac{V^2}{Z_N} \int \exp[-\beta U_N] \, dr^{N-2} \tag{1}$$

where $\beta = 1/kT$ and $Z_N = \int \exp[-\beta U_N] \, dr^N$ is the partition function.

Virial and compressibility equations express the pressure P and the reduced compressibility $\chi = (\partial \rho / \partial \beta P)_T$ in terms of simple integrals of $g(r)$:

$$\beta P = \rho - \frac{\rho^2}{6} \int g(r) \beta v'(r) r \, dr \tag{2}$$

$$\chi = S(0) = 1 + \rho \int (g(r) - 1) \, dr. \tag{3}$$

$S(0)$ represents the infinite wavelength limit of the structure factor $S(q)$.

It is always possible to write $g(r)$ as

$$g(r) = \exp[-\beta w(r)]. \tag{4}$$

This defines the so-called pair potential of mean force $w(r)$. Its name originates from the fact that the force $F(r) = -w'(r)$ is the mean force felt by particles 1 and 2, fixed and separated by the distance r, the average being taken over the configuration of the $N-2$ remaining particles $3, 4, \ldots$:

$$-\nabla_1 w(r_{12}) = \frac{\int (-\nabla_1 U_N) \exp[-\beta U_N] \, dr^{N-2}}{\int \exp[-\beta U_N] \, dr^{N-2}} = \left\langle \sum_{i=2,N} f_1(r_{1i}) \right\rangle = F_1(r_{12}). \tag{5}$$

Like $g(r)$, the mean force potential $w(r)$ is of free energy nature. It depends on ρ and T and implicitly contains many-body correlations. It is only at infinite dilution that the asymptotic law $g(r) = \exp[-\beta v(r)]$ applies and that $w(r)$ coincides with the direct pair potential $v(r)$. For the simple example of hard-sphere particles, $v(r)$ is exactly zero for non-overlapping spheres while $w(r)$ presents an attractive well near contact and oscillations at intermediate distances. This structure in w or in g is amplified as the density is increased and illustrates the short-range liquid order which results from packing constraints.

2.2. Mixtures and McMillan–Mayer theory of solutions

We now investigate solutions containing solvent molecules and solute colloid particles. Such mixtures are quite general: the solvent component may represent the organic or polar solvent itself as well as small solute molecules (salt, polymer, micelle, ...) which are added to the

solution in order to modify the colloid–colloid correlations. In the same way, the colloidal sub-system could be composed of different types of particles. The main idea of any statistical mechanical theory of solutions since McMillan–Mayer [17] consists in averaging over the degrees of freedom of the solvent molecules and deriving solvent-averaged potentials of mean force between solute particles. Note here that some particles like micelles in complex, mixed colloidal suspensions can be considered as belonging either to the solvent components or to the solute ones, depending on the degree of averaging and the level of analysis required.

To clarify the notation, we restrict ourselves here to binary mixtures composed of solvent (s) and colloid (c) particles. Generalization to solutions containing many solvent and/or solute species is straightforward. We assume that all particles interact via direct, bare, state-independent, pair potentials, $v_{ss}(r)$, $v_{cs}(r)$, $v_{cc}(r)$. The pair forces are represented by $f_{ij}(r) = -v'_{ij}(r)$. The system contains N_c colloidal spheres. The colloidal density N_c/V is denoted ρ_c. Rather than setting the solvent density $\rho_s = N_s/V$, it is better, both conceptually and in practice, to set the solvent chemical potential μ_s or the solvent activity $z_s = \exp(\beta\mu_s)/\Lambda_s^3$. This is equivalent to setting the density ρ'_s in a pure solvent reservoir which is in osmotic equilibrium with the solution through a semi-permeable membrane, allowing solvent molecules (but not colloids) to cross the membrane in order to equilibrate μ_s in both compartments.

The different pair distribution functions $g_{ij}(r)$ are expressed as statistical averages in this semi-grand canonical ensemble. For example [1]:

$$g_{cc}(r_{12}) = \frac{V^2}{\Theta} \sum_{N_s} \frac{z_s^{N_s}}{N_s!} \int \exp[-\beta U_{N_s+N_c}]\, \mathrm{d}\mathbf{r}^{N_s}\, \mathrm{d}\mathbf{r}^{N_c-2} \tag{6}$$

where the semi-grand partition function is

$$\Theta = \sum_{N_s} \frac{z_s^{N_s}}{N_s!} \int \exp[-\beta U_{N_s+N_c}]\, \mathrm{d}\mathbf{r}^{N_s}\, \mathrm{d}\mathbf{r}^{N_c}. \tag{7}$$

The total energy $U = U_{cc} + U_{cs} + U_{ss}$ is the sum of all pair interactions in the colloid–solvent mixture.

As for the monodisperse case, the definition

$$w_{cc} = -kT \ln(g_{cc}) \tag{8}$$

introduces the colloid–colloid pair potential of mean force, the average being taken now on the configurations of all solvent molecules and the $N_c - 2$ remaining colloids. w_{cc} must be viewed as a colloid + solvent-averaged pair potential.

Generalization of the virial (2) and compressibility (3) equations gives

$$\beta P = \rho - \frac{1}{6} \sum_{i,j} \rho_i \rho_j \int g_{ij}(r)\beta v'_{ij}(r)r\, \mathrm{d}\mathbf{r} \tag{9}$$

$$\chi = \left[\sum_{i,j} \frac{\sqrt{\rho_i \rho_j}}{\rho} S_{ij}^{-1}(0) \right]^{-1} = \left[1 - \sum_{i,j} \frac{\sqrt{\rho_i \rho_j}}{\rho} \hat{c}_{ij}(0) \right]^{-1}. \tag{10}$$

ρ_s must be understood as the averaged solvent density (which depends on ρ_c) while $\rho = \rho_c + \rho_s$ represents the total density.

$S_{ij}^{-1}(q)$ is the element ij of the matrix $\mathbf{S}^{-1}(q)$, the inverse of the matrix $\mathbf{S}(q)$, composed of the partial structure factors

$$S_{ij}(q) = \delta_{ij} + \hat{h}_{ij}(q) = \delta_{ij} + \sqrt{\rho_i \rho_j}\tilde{h}_{ij}(q). \tag{11}$$

$h_{ij} = g_{ij} - 1$ is the total correlation function and $\hat{h}_{ij}$ its Fourier transform, normalized by the density factor $\sqrt{\rho_i \rho_j}$. In the same way, $\hat{c}_{ij}$ represents the normalized Fourier transform of the

direct correlation function c_{ij}. Use of the Ornstein–Zernike (OZ) equation has been made in the second equality of (10). This equation, which reads in matricial form,

$$\mathbf{S}(\mathbf{1} - \hat{\mathbf{c}}) = (\mathbf{1} + \hat{\mathbf{h}})(\mathbf{1} - \hat{\mathbf{c}}) = \mathbf{1} \tag{12}$$

is the starting point of any theory based on integral equations. The exact closure to the OZ equation can be formally written as [1]

$$g_{ij}(r) = \exp[-\beta v_{ij}(r) + h_{ij}(r) - c_{ij}(r) + b_{ij}(r)] \tag{13}$$

where b_{ij} represents the so-called bridge function. Neglecting b_{ij} defines the HNC integral equation. Further linearization of the exponential factor beyond the contact (at distances larger than the hard-sphere diameter σ_{ij}) leads to the MSA equation, $c_{ij}(r) = -\beta v_{ij}(r); r > \sigma_{ij}$.

The McMillan–Mayer theory of solutions gives for the reduced osmotic compressibility [18]

$$\chi_{osm} = \left(\frac{\partial \rho_c}{\partial \beta \Pi}\right)_{osm} = S_{cc}(0). \tag{14}$$

Π represents the osmotic pressure, i.e. the difference between the absolute pressures in the solution P and in the reservoir P'. The thermodynamic derivative is expressed in the conditions of osmotic equilibrium, namely at T and μ_s (or ρ_s') constant. χ_{osm} depends explicitly only on the colloid–colloid pair correlations, in contrast to the full compressibility χ (10), and is formally equivalent to the compressibility (3) of the monodisperse gas of solute particles.

2.3. Potentials of mean force

In general, the colloidal particles are much larger and heavier than the solvent molecules. As a consequence, most of the experimentally measurable quantities like the scattered intensity are sensitive only to the correlations between colloids. It is thus tempting and fruitful to formally regard the two-component mixture as a one-component system composed of colloids interacting via an effective, solvent-averaged N_c-body potential of mean force $W_{N_c}(r^{N_c})$ [17, 19]. The idea of this approach is to decompose the full statistical averages of the mixture in two successive steps [20, 21] (this decomposition is explicitly used in some numerical simulations [22]): for a given configuration of the colloidal particles (r^{N_c}), the average over the degrees of freedom of the solvent molecules is performed in the non-homogeneous space imposed by the presence of the colloids, defining the solvent-averaged potential $W_{N_c}(r^{N_c})$ and the force felt by each colloid $\boldsymbol{F}_i(r^{N_c}) = -\nabla_i W_{N_c}$. Then, the statistical average over the colloidal degrees of freedom is performed in the one-component system with the Boltzmann factor $\exp(-\beta W_{N_c})$. Note that, in theory, as long as the static properties are concerned, this one-component model (OCM) exactly reproduces the properties obtained with the two-component approach, which treats in parallel and on an equal footing the colloid and the solvent degrees of freedom (this would also be true for the dynamic properties but only in the adiabatic limit where the solvent molecules relax instantaneously around the moving colloids). In practice, this decomposition is a powerful way to exhibit fundamental concepts of interaction and correlation in mixed systems and to derive simple, approximate but accurate expressions for W used as inputs in the simple OCM. Different expressions for $W_{N_c}(r^{N_c})$ can be defined, which differ only by an additive constant which is irrelevant for the colloid correlations or forces but which is important for the thermodynamics of the solution.

Equating the semi-grand potential $\Omega(T, V, \mu_s, N_c) = F - \mu_s N_s = -PV + \mu_c N_c$ (F is the free energy) in the two- and one-component approaches gives the fundamental definition [21, 23]

$$\exp[-\beta W_{N_c}] = \sum_{N_s} \frac{z_s^{N_s}}{N_s!} \int \exp[-\beta U_{N_s+N_c}] \, \mathrm{d}r^{N_s} = \mathrm{e}^{-\beta \Omega_s'} \langle \exp[-\beta(U_{cc} + U_{cs})] \rangle_s \tag{15}$$

where the first term in the right-hand side of (15) represents the partition function of the pure solvent reservoir (of the same volume V) with $\Omega_s' = -P'V$ and the second term (in brackets) can be viewed as the mean Boltzmann factor $\langle \exp[-\beta\phi_{N_c}]\rangle_s$ (with $\phi = U_{cc} + U_{cs}$) of a test complex, N_c-body particle introduced randomly into the solvent system.

By construction, the thermodynamics and the spatial correlations (at any order) between colloids in the OCM with the potential (15) are identical to those obtained in the original two-component system. For example, the pair distribution function g_{cc} (6) can be reproduced with the OCM expression (1) with U_N replaced by W_{N_c}. Note that W_{N_c} does not vanish in the limit of very large inter-colloid distances. In other words, it contains familiar two-, three-, ... multi-body (colloid) terms as well as zero- and one-body terms which are important for the thermodynamics of the solution [20, 21, 23]. Each term can be expressed as a diagrammatic expansion in powers of z_s. As far as the spatial correlations are concerned, the special zero- and one-body terms can be discarded. The new definition, which differs from (15) by an additive constant, independent of the colloidal positions, reads [24]

$$\exp[-\beta W_{N_c}] = \frac{\langle \exp[-\beta\phi_{N_c}]\rangle_s}{\langle \exp[-\beta\phi_1]\rangle_s^{N_c}}. \tag{16}$$

The term in brackets in the denominator represents the mean Boltzmann factor of a test isolated colloid immersed in the solvent. At large inter-colloid distances, the mean Boltzmann factor in the numerator can be factorized and the potential of mean force in (16) vanishes, as required. At low colloidal density, the colloids interact mainly by pair and W can be restricted to the sum of pair potentials W_2. In the limit of zero colloidal density, w_{cc} in (8) coincides with W_2 (we will see later how this simple law breaks down for salt-free charged colloidal systems). At finite density, higher order terms become important and W is no longer pairwise additive.

From any of the two definitions for W, the mean force applied to a colloid i in the configuration (r^{N_c}) can be decomposed as

$$\boldsymbol{F}_i(r^{N_c}) = -\nabla_i W_{N_c} = \boldsymbol{F}_{ci} + \int \rho_s(\boldsymbol{r}) f_{sc}(|\boldsymbol{r} - \boldsymbol{r}_i|)\, \mathrm{d}\boldsymbol{r}. \tag{17}$$

The first term is the direct force $-\nabla_i U_{cc}$, i.e. the sum of pair forces f_{cc} coming from the colloid neighbours. The second term arises from the solvent particles whose local density inside the inhomogeneous solution, around the colloids, is denoted by $\rho_s(\boldsymbol{r})$. In principle, expression (17) for the mean forces does not bring more information than the potential of mean force W. In practice, the free energy route and the force route are both useful and complementary to fully understand the various couplings inside the solution.

Where the thermodynamics of the solution is concerned, the solvent contribution must be taken into account through the zero- and one-body terms in the potential of mean force (15). From the equivalent pressure point of view, the virial equation (9) of the solution becomes, using the two successive steps in the averaging,

$$P = \rho kT - \frac{1}{3V}\left\langle \sum_{i\in c,s} \boldsymbol{r}_i \nabla_i U_N \right\rangle_{s,c} = \rho kT + \frac{1}{3V}\left\langle \sum_{i\in c} \boldsymbol{r}_i \cdot \boldsymbol{F}_i \right\rangle_c + \frac{1}{3V}\left\langle \int \boldsymbol{r} \cdot \boldsymbol{f}_s(\boldsymbol{r})\rho_s(\boldsymbol{r})\, \mathrm{d}\boldsymbol{r} \right\rangle_c$$

$$+ \frac{1}{6V}\left\langle \iint |\boldsymbol{r} - \boldsymbol{r}'| v_{ss}'(|\boldsymbol{r} - \boldsymbol{r}'|)\rho_{ss}(\boldsymbol{r}, \boldsymbol{r}')\, \mathrm{d}\boldsymbol{r}\, \mathrm{d}\boldsymbol{r}' \right\rangle_c \tag{18}$$

while the OCM virial equation (2) would give

$$\beta P = \rho_c kT + \frac{1}{3V}\left\langle \sum_{i\in c} \boldsymbol{r}_i \cdot \boldsymbol{F}_i \right\rangle. \tag{19}$$

Expression (18) for the absolute pressure contains the virial pressure of the solvent in the non-homogeneous space characterized by (r^{N_c}). $\boldsymbol{f}_s(\boldsymbol{r}) = -\nabla u_s(r^{N_c}, \boldsymbol{r})$ represents the external

force due to all colloids, $u_s(\mathbf{r}^{N_c}, \mathbf{r}) = \sum_{i \in c} v_{cs}(|\mathbf{r} - \mathbf{r}_i|)$ the external potential and ρ_{ss} the two-particle density. The *osmotic* pressure Π of the solution is rigorously given by the difference between (18) and the corresponding expression for the pure solvent. To what extent is this difference correctly recovered by the OCM expression (19)? This usually fruitful identification of the colloidal 'gas' pressure (19) with the osmotic pressure of the solution Π is not exact following the virial route and must be applied with caution. In particular, it fails to account for the counter-ion contribution in charged colloidal systems (see section 4). This should be opposed to the more universal OCM compressibility route, which *always* gives the exact osmotic pressure through (14).

Closing this section, one could investigate the ideal case where the solvent molecules do not interact with each other, $v_{ss} = 0$, but interact only with the colloids [21]. The (perfect gas) pressure in the reservoir is $P' = \rho'_s kT$. Since the solvent molecules are uncorrelated, the partition function of the solvent in the non-homogeneous fluid can be factorized. The final result for the potential of mean force reads [21]

$$W_{N_c} = U_{cc} - P'\vartheta(\mathbf{r}^{N_c}) \tag{20}$$

where the interaction volume is

$$\vartheta = \int e^{-\beta u_s}(\mathbf{r}^{N_c}, \mathbf{r}) \, d\mathbf{r} \tag{21}$$

in the first definition (15), and is

$$\vartheta = \int [e^{-\beta u_s(r^{N_c}, r)} - 1 - N_c(e^{-\beta u_s(r^1, r)} - 1)] \, d\mathbf{r} \tag{22}$$

in the second definition (16). The local solvent density which monitors the mean forces (17) is simply

$$\rho_s(\mathbf{r}) = \rho'_s e^{-\beta u_s(r^{N_c}, r)}. \tag{23}$$

In the real case, expression (20) gives the correct behaviour only to first order in z_s or ρ'_s.

2.4. Effective, solvent-averaged, pair potential

In general, the N_c-body potential of mean force is not pairwise additive and depends on the relative position of all colloids. This prevents a simple visualization and a clear understanding of the solvent effects. For example, it is difficult to deduce, from the force felt by each colloid in a given configuration, the extent to which the colloids 'on average' repel or attract one another in solution. In order to overcome this difficulty, it is tempting to write formally W_{N_c} as a *sum* of *pair* contributions

$$W_{N_c}(\mathbf{r}^{N_c}) = \sum_{i<j} v_{cc}^{eff}(r_{ij}) \tag{24}$$

and introduce the so-called effective, solvent-averaged, colloid–colloid *pair* potential $v_{cc}^{eff}(r)$. Again, (24) is an approximation. A pair description alone is not able to reproduce the colloidal forces and all colloid–colloid correlations resulting from the original full potential of mean force W_{N_c}, whatever the form of $v_{cc}^{eff}(r)$. Nevertheless, it should be sufficient to reproduce at least the *pair* correlations. This leads to the following *rigorous* definition which seems to be the most natural and interesting one [25] and has been intensively applied with success in charged systems since the early 1980s [26–29]:

> $v_{cc}^{eff}(r)$ is the *pair* potential which would lead, within the OCM and the pairwise additivity assumption, to the same colloid–colloid pair distribution function $g_{cc}(r)$ as obtained within the two-component model, at identical temperature and colloidal density. (25)

In practice, one must first solve the mixture problem characterized by the pair potentials $v_{ij}(r)$ or, equivalently, the OCM with the N_c-body potential of mean force. Then, the pairwise additive OCM is solved in the reverse of the usual way, the (effective) pair potential being extracted from the known pair correlations. Note that the uniqueness of the solution to this inverse problem has been established [30]. The effective potential so defined is exactly the potential extracted from standard fits of experimental scattering spectra $I(q)$.

In principle, there is no more information in $v_{cc}^{eff}(r)$ than in $g_{cc}(r)$ or $S_{cc}(q)$. In contrast to W_{N_c}, v_{cc}^{eff} does not represent some intermediate function in a two-step averaging (one must integrate over the colloidal degrees of freedom before deriving it). Nevertheless, in practice, it is a powerful concept, which clearly illustrates how the solvent monitors the effective interaction between colloids. In particular, the sign of v_{cc}^{eff} indicates whether the colloids feel a repulsion or an attraction from their neighbours, on average. Moreover, analytical, approximate albeit accurate expressions for v_{cc}^{eff} can be deduced in various systems.

v_{cc}^{eff} can be viewed as a solvent-averaged or semi-mean force pair potential. It differs from W_2 and depends on the colloidal density since it implicitly contains partially averaged many-body interactions. By construction, it leads exactly to the same *pair* correlations as in the original system but it is in general insufficient to give the correct n-body correlations of higher order, $g_{cc}^{(3)}, \ldots$. Fortunately, this weakness does not affect the thermodynamics using the *compressibility* route (14). In particular, if one approaches a liquid–gas spinodal line or critical point in the phase diagram of the two-component system, χ_{osm} and $S_{cc}(0)$ present diverging values, which automatically imply the existence of attractions in v_{cc}^{eff} near this thermodynamic state.

We are now left with three kinds of colloid–colloid pair potential in the mixture, v_{cc}, v_{cc}^{eff} and w_{cc}, which must not be confused. The two last depend on the thermodynamic state and differ by the degree of averaging. v_{cc}^{eff} is a solvent-averaged potential while w_{cc} is the solvent + colloid-averaged potential (of mean force). For example, in hard-sphere mixtures, the former will present negative values near contact due to the osmotic pressure of the small spheres against the two investigated colloids (this local osmotic pressure being perturbed by the colloidal environment) while the latter will present negative values due to the osmotic pressure of the solvent as well as colloid particles (two mixed depletion effects). In the absence of solvent, v_{cc}^{eff} and v_{cc} coincide while w_{cc} contains the usual one-component contributions of free-energy origin. In the opposite limit of zero colloidal density, v_{cc}^{eff} and w_{cc} coincide (except, again, for the important case of salt-free charged systems) and represent the interaction between two isolated colloids immersed in the solvent.

In practice, the usual procedure for extracting the effective pair potential starts by mapping the two-component OZ equation (12) onto a one-component one [25]. Identifying g_{cc} in both models gives for the OCM effective direct pair correlation function

$$\hat{c}_{cc}^{eff} = \hat{c}_{cc} + \frac{\hat{c}_{cs}^2}{1 - \hat{c}_{ss}}. \tag{26}$$

Once an integral equation within the OCM has been chosen, the effective potential is directly deduced from $g_{cc}(r)$ and $c_{cc}^{eff}(r)$. In practice, the integral equations used in both models are approximated and it is necessary and sufficient at this level of approximation to use the same integral equation in the OCM as in the mixture [27–29] (this guarantees at least that direct and effective potentials coincide in absence of solvent).

Comparing the diagrammatic expansions of the pair distribution function g_{cc} in the two-component mixture characterized by T, ρ_c, z_s, v_{ij} and in the OCM characterized by T, ρ_c, v_{cc}^{eff}, and identifying the terms of same order in ρ_c, gives the first diagrams listed in figure 1
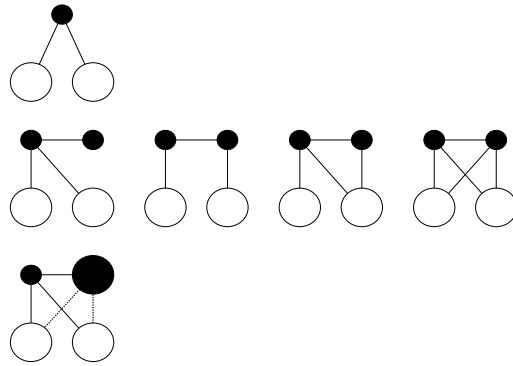
Figure 1. First diagrams in the expansion of the colloid–colloid effective pair potential $v_{cc}^{eff}(r)$. The small black symbols are field solvent particles, weighted with solvent activity z_s. The solid lines represent Mayer function links $f_{ij} = \exp(-\beta v_{ij}) - 1$. At this level of expansion, $\rho_s/z_s = 1 + \rho_c \int f_{cs}(r)\,dr$. In the last diagram, the large black symbol is a field colloid particle and the dotted lines represent $1 + f_{cc} = \exp(-\beta v_{cc})$ links.

for the effective potential v_{cc}^{eff}. Note the presence of diagrams involving colloid neighbours which illustrates the ρ_c-dependence of this effective pair potential.

The leading, three-body (2 colloids+1 solvent) term is given by (20),(22) and corresponds to the first diagram in figure 1:

$$v_{cc}^{eff}(12) = v_{cc}(12) - kT\rho_s' \int (e^{-\beta v_{cs}(13)} - 1)(e^{-\beta v_{cs}(23)} - 1)\,d\mathbf{r}_3. \qquad (27)$$

The corresponding expression using the force route (17) is

$$-v_{cc}^{eff\prime}(12) = \mathbf{f}_{cc}(12) + \rho_s' \int \mathbf{f}_{cs}(13)\,e^{-\beta(v_{cs}(13)+v_{cs}(23))}\,d\mathbf{r}_3. \qquad (28)$$

The integrals in (27) and (28) represent the first effect of the solvent molecules on the potential/force between colloids. They can be derived and understood in an intuitive way: the potential expression represents the difference in free energy of the inhomogeneous solvent subsystem between configurations characterized by r_{12} and by $r_{12} = \infty$. The force expression is even more obvious and represents the integrated force coming from the solvent molecules which are located around the two colloids. Anticipating the discussion in the next sections, one already notes that both cs repulsion and attraction lead at this level of approximation to an effective attraction between colloids. In the former case, there are less solvent molecules in the interstitial region between the colloids than in the opposite directions since, there, the solvent is repelled by the two colloids at the same time. This asymmetry in solvent population results in a force which pushes the colloids towards each other, namely in an effective attraction of depletion origin. The analogous discussion in terms of potential is related to the convexity of the exponential function: when the colloids are close to each other, the solvent molecules are less frustrated by the repulsion coming from the colloids (compared to the large separation configuration), their partition function in the inhomogeneous system is higher and their free energy is lower, which means that the configuration is more favourable and the effective potential is negative. In the latter case of cs attraction, the situation is reversed: more solvent molecules accumulate in the interstitial region (simultaneous attraction from both colloids), which results in an effective attraction between colloids, this time of bridging origin.

The leading diagram (27) is sufficient to understand the interaction between colloids at low solvent density as it is sufficient to give the third virial coefficient in monodisperse systems.

At higher solvent activity, many body correlations take place, more diagrams must be included and the situation becomes less obvious and requires careful analysis.

3. Colloidal interactions in neutral systems

3.1. Hard-sphere mixtures: depletion and structural forces

The simplest example of a colloid/solvent system is the hard-sphere mixture (diameters σ_s and σ_c), characterized by the pair potentials

$$\beta v_{ij}(r) = +\infty \qquad r < \sigma_{ij} = (\sigma_i + \sigma_j)/2$$
$$= 0 \qquad r > \sigma_{ij}. \tag{29}$$

This athermal system is governed by correlations of entropic (excluded volume) origin. The main effect, the depletion attraction between large balls due to the osmotic pressure exerted by the small ones, was first introduced by Asakura and Oosawa [31]. In the last few years, the hard-sphere mixtures have been the subject of beautiful experimental and theoretical studies, focusing on the force acting on the colloids as well as on the phase separation which could result from the depletion attraction (see [32], [23] and references therein). Experiments mainly concern mixtures of large neutral colloids and short non-adsorbing polymers immersed in *theta* solvent. The polymer coils are seen as small spheres, more or less penetrable one to each other.

In the pure-hard sphere mixture, the particles feel each other only during collisions (at contact). The force exerted by a solvent sphere on a colloid can be written as $kT\delta(r - \sigma_{cs})$. Consequently, the volume integral which gives the solvent force acting on each colloid (17) reduces here to a surface integral [33]

$$F_i(r^{N_c}) = - \int_{S_i} \rho_s(S)kT \, dS. \tag{30}$$

S_i represents the sphere centred on r_i, of diameter σ_{cs}. The surface vector dS points outwards this sphere. Due to the presence of the colloidal neighbours around i, the solvent density at contact $\rho_s(S)$ is not spherically symmetric. As a consequence, the unbalanced osmotic pressure of the solvent molecules $\rho_s(S)kT$ against the ith sphere results in a net force F_i.

To first order in z_s or ρ_s' (or in the ideal case where the solvent molecules do not feel each other, $\sigma_{ss} = 0$), the local density $\rho_s(r)$ coincides with ρ_s' in the interstitial regions accessible to the small balls and is zero elsewhere [21]. The surface force reduces to

$$F_i(r^{N_c}) = -\rho_s'kT \int_{S_i\,'free'} dS. \tag{31}$$

S_i 'free' represents the portion of surface S_i accessible to the solvent molecules (not excluded by the volume of the colloid neighbours). Equivalently, the N_c-body potential of mean force reduces in the same limit to

$$W_{N_c} = -\rho_s'kT\vartheta_{free}(r^{N_c}) \tag{32}$$

where the interaction volume coincides with the real free volume offered to the solvent molecules in the fixed (r^{N_c}) configuration (minus the free volume at infinite separations).

The origin of the depletion attraction is now clear (figure 2(a)): when two colloids 1 and 2 approach each other at $r_{12} < 2\sigma_{cs} = \sigma_c + \sigma_s$, the two excluded volumes V_1 and V_2, of radius σ_{cs}, forbidden to the solvent, begin to overlap, which means that the free volume increases by the quantity $V_1 \cap V_2$, and the entropic pair potential W_2 is equal to $-\rho_s'kT V_1 \cap V_2$. Using the equivalent force picture, the presence of particle 2 in the vicinity of particle 1 prevents the solvent molecules from going between 1 and 2. The existence of this depletion region breaks
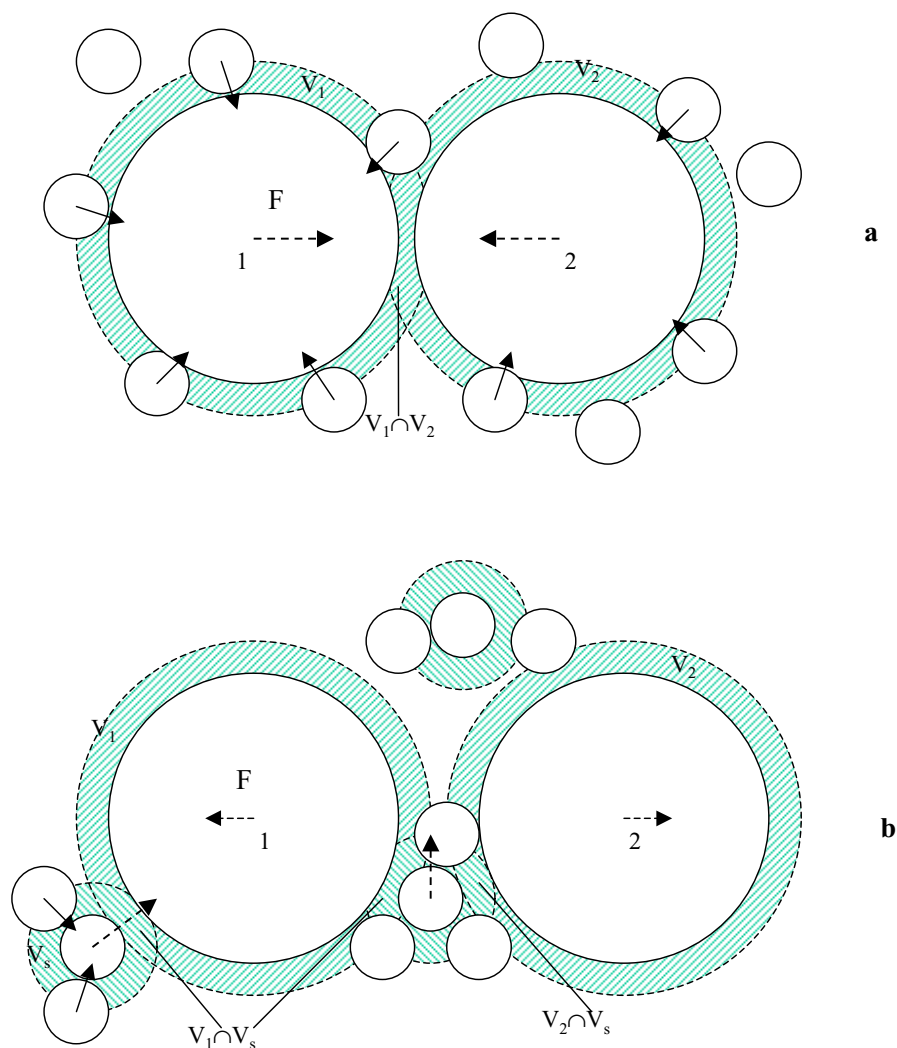
Figure 2. Schematic representation of excluded volume correlations in asymmetrical hard-sphere mixtures. The dotted zones are forbidden regions for the solvent particles, the solid arrows indicate local solvent osmotic pressure forces, the dashed arrows represent effective forces. (a) Bare, first order depletion attraction. (b) Second order structural repulsion: increase of the solvent density near colloidal surfaces enhanced in the interstitial region (see text).

the osmotic pressure balance around 1 and the solvent molecules located in the direction opposite to 2 push particle 1 against particle 2.

For two colloids in contact ($r_{12} = \sigma_c$), the first diagram gives $\beta W_2 = -\phi_s(1 + \frac{3}{2}\sigma_c/\sigma_s)$ and $\beta F = -(\pi/4)\rho'_s\sigma_s(2\sigma_c + \sigma_s)$ [34]. At constant volume fraction occupied by the solvent ϕ_s, the depletion attraction becomes shorter range and deeper at contact when the solvent molecules become smaller [35].

In general, the free volume accessible to the solvent is not pair-wise additive. For example, in the presence of three approaching colloids 1, 2 and 3, the gain in free volume (compared to the infinite separation situation) is $V_1 + V_2 + V_3 - V_1 \cup V_2 \cup V_3$

$\equiv V_1 \cap V_2 + V_1 \cap V_3 + V_2 \cap V_3 - V_1 \cap V_2 \cap V_3$ and, due to the extra, three-body term, is smaller than the sum of the previous two-body volumes [36]. The existence of this three-body repulsion indicates that the *effective* depletion pair attraction decreases in general with increasing volume fraction (this shows up in the repulsive last diagram of figure 1, involving three colloids). Meanwhile, for large size ratio σ_c/σ_s (larger than $2\sqrt{3} + 3 \approx 6.5$), the intersection volume $V_1 \cap V_2 \cap V_3$ is empty, even for three colloids in contact, and the depletion attraction is additive by pairs, at least to first order in the solvent density.

When the volume fraction of the solvent sub-system becomes appreciable, the bare depletion picture is not sufficient to describe the colloid interactions and diagrams of higher order, involving 2, 3, ... solvent molecules must be taken into account [37, 38]. The solvent-solvent excluded volume ($\sigma_{ss} \neq 0$) induces a short-range liquid order in the solvent liquid which is perturbed near a colloidal surface. The main effect is the appearance of an 'adsorbed' solvent layer (of higher density than the bulk solvent density) around each colloid. The origin of this layer is still entropic and can be explained as a depletion effect, this time between one colloid and one solvent sphere. Following the same reasoning as before (see figure 2(b) for a schematic picture), when one particular solvent sphere s is located near a colloidal wall 1 ($r < \sigma_{cs} + \sigma_s$), a depletion region appears between them which is excluded to the solvent neighbours, resulting in a net osmotic force which pushes the solvent sphere against the wall. In other words, the free volume accessible to the solvent liquid is increased when the excluded spherical volumes V_s and V_1 of radius σ_s and σ_{cs} centred on the solvent and colloid positions respectively, begin to overlap. The induced solvent layer has a thickness of σ_s. As a first effect of the extra-solvent density, the bare depletion attraction between touching colloids increases. More importantly and subtly, this accumulation of solvent near a surface is enhanced in the interstitial region between two approaching colloids 1 and 2 ($r_{12} < \sigma_c + 2\sigma_s$). Indeed, within this region, the solvent sphere maximizes the gain in free volume for its solvent neighbours, $V_s \cap V_1 + V_s \cap V_2$. Or, using the pressure picture, the solvent sphere located at the entry of the 'funnel' feels a net osmotic force along the mid-plane between 1 and 2 which pushes it in the direction of the exit of the funnel. Both routes indicate that the local solvent density around the two colloids is higher between them than in the opposite direction. According to (30) for the mean force, this results in a repulsion between colloids which adds to the bare depletion attraction (in other words, when two colloids approach each other, their adsorbed solvent layers begin to overlap the hard cores and the partial destruction of them costs in free energy). At separations $\sigma_c + \sigma_s < r_{12} < \sigma_c + 2\sigma_s$, the bare depletion vanishes and the new repulsion dominates. This effect of order $\rho_s'^2$ corresponds to the diagrams of the second line in figure 1.

The previous analysis helps us to understand why the interaction between large balls in an ocean of small ones presents at high volume fraction a depletion attraction near contact followed by oscillations of period σ_s between domains of repulsion and attraction (figure 3). This behaviour, similar to what happens in monodisperse hard-sphere systems, is the signature of the liquid order of the underlying fluid and of its alteration by the presence of one or two colloids in the neighbourhood.

Direct measurements of hard-sphere depletion pair interactions have been performed between curved mica surfaces in non-aqueous liquids [39] (SFA) and between polystyrene colloids and flat glass surfaces in nonionic polymer solutions [40] (TIRM). Indirect experimental evidence for the depletion is generally deduced from the stability of hard-sphere mixtures with respect to phase separation [41]. Concerning the theoretical prediction of phase diagrams, one must keep in mind that the strength of the depletion attraction determined at *zero* colloidal density is in principle not sufficient to determine the precise location or even
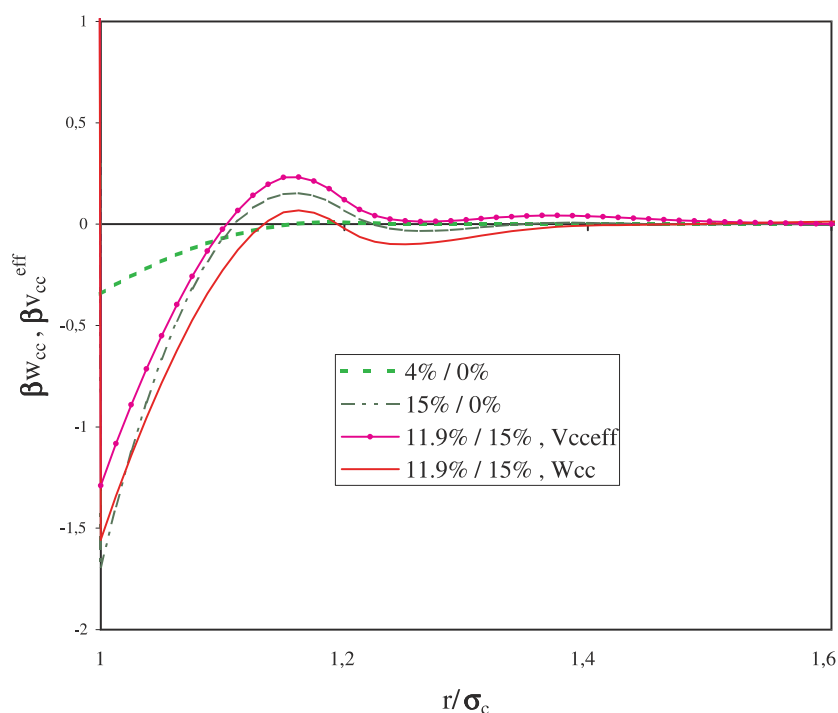
Figure 3. Effective $v_{cc}^{eff}(r)$ and mean force $w_{cc}(r)$ pair potentials between colloids in pure hard-sphere mixtures: depletion + structural forces. $\sigma_c/\sigma_s = 5$. The curves are labelled with their volume fraction composition Φ_s, $\Phi_c = 4\%$, 0%; 15%, 0%; 11.9%, 15%. The last two cases correspond to the same solvent activity or solvent density in the reservoir $\Phi_s' = 15\%$. BHP integral equation [123] in the two-component and effective one-component models.

to guarantee the existence of the liquid–gas or fluid–crystal transition. Indeed, the effective pair potential becomes less attractive in general for increasing colloidal volume fraction due to the 3, 4, . . .-colloid contributions in the N_c-body potential of mean force (figure 3). At high size ratio, the non-additivity character appears only at high solvent volume fraction (the solvent molecules located in the gap between colloids 1 and 2 and those located in the gap between colloids 2 and 3 are coupled only in diagrams of high order, involving many solvent balls) and the pairwise additivity approximation should be valid at lower solvent density. The reader interested by this issue is referred to a recent simulation work [23], which unambiguously proves the existence of additive hard-sphere phase separation in this regime.

Starting from the reference case of hard-sphere mixtures, we will now investigate step by step the presence of extra, soft interactions between the various components. Four basic cases can be distinguished.

3.2. Colloid–solvent repulsion: enhanced, longer-range, depletion

A soft repulsion, of range $d \gg \sigma_s$, between colloid and solvent particles is added to the previous hard-sphere interactions. As a consequence, a depletion layer of solvent develops around each colloid (negative adsorption) which leads, following the same mechanism as before, to an attraction between colloids. The interaction volume (22) cannot be simply identified with

a real free volume now but the resulting interaction is very similar to that obtained in the pure hard-sphere case. Roughly speaking, the hard-spheres results can be applied with the colloid–solvent contact distance σ_{cs} replaced by a renormalized value of the order $\sigma_c/2 + d$ (the case of pure hard-sphere mixtures with positive nonadditivity in diameter has recently been considered in [42]). Thus, the enhanced depletion may be important even at low hard-sphere volume fraction ϕ_s.

This simple analysis allow us to explain why two hydrophobic surfaces, carrying groups which repel water molecules, attract each other [43]. The strength of this hydrophobic force may be sensitive to the temperature [44]. Its range, linked to the range of the colloid–solvent repulsion, is generally limited to a few nanometres in surface–surface separation.

Another illuminating application can be found in mixtures of large and small *charged* objects of same sign, the small component playing the role of the solvent. The particles interact via (ion-averaged) screened coulombic repulsions, which decay as $\exp(-\kappa r)/r$. The colloid–solvent repulsion induces a deep attraction between colloids, which adds to and sometimes dominates the direct repulsion [37]. This depletion of electrostatic origin has been observed in various systems like mixtures of SDS micelles and large oil droplets stabilized by a SDS surfactant layer [45, 11] (optical observation), crossed mica cylinders coated with an adsorbed bilayer of CTAB and immersed in a CTAB micellar solution [46] (SFA experiments) and polystyrene particle near a glass plate in presence of silica particles or charged polymers [47] (TIRM). The depth of the attraction is monitored by the depletant concentration (in ρ_s to leading order) while the range is related to the large Debye length κ^{-1}.

In the same way, the coulombic repulsion between large and small colloids in highly deionized bidisperse charged latex suspensions induces a 'charge ordering' even at low volume fraction which can be observed in x-ray or neutron scattering experiments [48, 49]. The contrast match technique makes it possible to determine the pair correlations among particles of one of the two components (viewed here as the 'colloid' component). The partial intensity curves can be interpreted in terms of effective pair potentials (25) which present a clear electrostatic depletion due to the hidden particles of the other ('solvent') component [49].

We next proceed with a slight digression. It happens in some charged colloidal systems that, despite intensive cleaning through dialysis or ion exchange resin, small charged pieces of material remain in the solution between the colloids. An important example is constituted by latex systems where the surface of the lattices may release charged polymers of low mass in the bulk [6]. These new particles are not small enough to cross a dialysis membrane. Moreover, since the release seems to result from an equilibrium between surface and bulk, the solution will always contain the extra component even after careful cleaning. The polymers are negligible with respect to the mass fraction of colloids. They do not contribute (at least directly) to any scattered intensity and cannot be seen by optical visualization. On the other hand, they contribute to and even dominate the total number of particles as can be observed in osmotic pressure experiments [6]. More importantly, in highly deionized solutions, the ionic strength is kept very low, the Debye length is large, much larger than the real size of the small molecules, and the effective, electrostatic, volume fraction of the charged polymers may be large, inducing a strong depletion attraction between colloids. This effect could explain [50] non-classical behaviours observed in highly deionised monodisperse latex systems [51].

3.3. Solvent–solvent repulsion: oscillating structural force

If the solvent molecules repel each other through a soft repulsion of range $d \gg \sigma_s$, they tend to accumulate near inert colloidal surfaces and a repulsion at contact followed by oscillations will appear at high solvent density in the colloid–colloid effective potential. This structural

force (in ρ_s^2 to leading order) is similar to that described in hard-sphere mixtures although the softness of the *ss* repulsion somewhat damps the oscillations of period d. It could be clearly identified in mixtures of large *neutral* colloids and small charged micelles where the absence of colloidal charge guarantees the absence of direct repulsion and indirect depletion attraction between colloids. When the colloids become charged (again of the same sign as the solvent), all effects add up and the resulting interaction between colloids presents complex structures which depend on the size and charge ratios and on the solvent density, as seen in the experiments mentioned above [45–49].

Before closing sections 3.2–3.3 on depletion and anticipating the analysis of charged systems in section 4, it is important to note here that the description of charged solvent effects solely in terms of electrostatic depletion attraction between colloids must be used with caution at low ionic strength. In that regime, the effect of the solvent particles on the colloid-colloid effective interaction is less of depletion than of screening nature. In practice, this means that the diagrammatic or virial expansion is only slowly convergent and keeping only the first leading terms could lead to predicting a strong attraction where the correct ion + solvent-averaged interaction is purely repulsive (see the discussion at the end of 4.1).

3.4. Colloid–solvent attraction: steric, stabilizing repulsion + bridging attraction

What happens when the solvent molecules present an affinity for the colloidal surfaces? The direct *cs* potential is now the sum of the hard-sphere repulsion and of a soft attraction. As a consequence, the leading expression for the effective *cc* potential will contain three contributions, (i) the bare hard-sphere depletion attraction, (ii) a steric repulsion and (iii) a bridging attraction at larger distances. The physical picture is trivial: when the *cs* attraction is turned on, an adsorbed solvent layer will appear around each colloid. When two particles approach each other, the layers first begin to overlap. The local solvent density increases, which induces a bridging attraction (ii) (note that if the adhesion attraction is highly directional, the solvent molecules in the gap cannot stick to two surfaces at the same time and the bridging effect disappears). The separation still decreasing, the layers are now perturbed by the internal hard cores and are partially destroyed. The intersticial density decreases by volume exclusion, there is a loss of attractive energy (cost in free energy) and this frustration induces a so-called 'steric' repulsion at short distance (iii) which rapidly overcomes the bare depletion (i), even at low affinity (see figure 4).

This kind of repulsion is the basis of any steric stabilization of colloidal suspensions due to the presence of adsorbing molecules [9]. In the limit of strong binding, the adsorbed layer can be viewed as an additional hard core which prevents the colloids from coming into true contact. Examples of stabilizing agents are (adsorbing) polymers, small organic complexant molecules or some organic or polar solvents. In the important case of water as a solvent, hydrophilic surfaces are stabilized through the so-called hydration force. Before going into detail in these examples, it is first necessary to complete the study with the last basic case of direct interaction.

3.5. Solvent–solvent attraction: modulation of steric and hydration forces

In the case of solvent–solvent attractions of range d, the frustration felt by the solvent in the vicinity of passive hard-core volumes induces a depletion layer around colloids. This depletion, enhanced in the interstitial regions, induces as before an effective attraction between colloids (figure 4). This means that passive surfaces behave as solvophobic when immersed in a solvent with *ss* attraction. The range of the depletion attraction is usually of the order of d, except
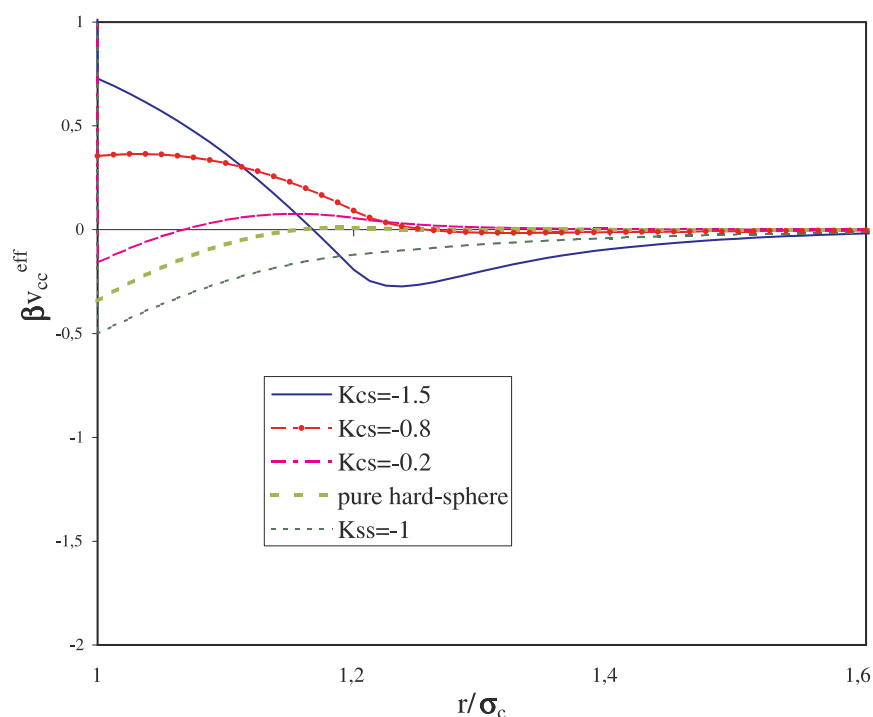
Figure 4. Effective colloid–colloid pair potential $v_{cc}^{eff}(r)$ in hard-sphere mixtures with additional colloid–solvent or solvent–solvent direct attraction: steric + bridging or solvophobic forces. $\sigma_c/\sigma_s = 5$, $\Phi_s = 4\%$, $\Phi_c = 0$. $\beta v_{cs}(r)$ and $\beta v_{ss}(r)$ are Yukawa potentials of range $d = \sigma_s/2$ and depth at contact K_{cs} and K_{ss}, respectively. BHP integral equation.

in the limit of a solvent very close to its liquid–gas spinodal line or critical point where it is related to the large correlation length of the fluid [52].

It is now possible to analyse the complex behaviours observed in real suspensions which combine affinity of the solvent for the surfaces and solvent–solvent attraction or repulsion.

For macroscopic surfaces or micrometric colloids, steric stabilization involves most often adsorbing polymers [53]. The steric layer is due to irreversible grafting or reversible physi- or chemisorption. The polymer-average potential between colloids and the stability of the solution will depend on the strength of the adhesion, on the temperature or on the quality of the real solvent for the polymer (steric, entropic repulsion enhanced in good solvent, attraction in bad solvent) and on the degree of coverage (bridging attraction at intermediate value) [9]. Although the precise form of the interaction involves the polymeric nature of the molecules, the simple analysis described above is usually sufficient to qualitatively explain most of the behaviours.

For nanometric colloids, polymers are less adapted due to the formation of bridging necklaces [54] and to the important volume fraction occupied by the thick adsorbed 'layers' [55]. A better candidate for steric stabilization involves small complexant molecules. The complexing shell plays the role of a 'double sided tape': the inner side is strongly adhesive to bind to the colloidal surface and blocks its reactivity, while the outer side may induce a weak attraction between covered stabilized particles [56].

The short-range, strong hydration repulsive force observed in colloidal and biological aqueous solutions results from complex couplings between water–surface and water–

water interactions (see the recent review [57]). The presence of dipole, quadrupole, ..., polarizability in the water molecule induces highly directional (hydrogen bonds) water–water attractions favouring tetrahedral icelike configurations. A surface can be considered as hydrophilic only if 'it likes water more than water likes water'. This is the case of materials like silica or lecithin or surfaces carrying hydrophilic groups (H-bonding groups, bound ions, ...). The strong binding of H_2O molecules (surface hydration) guarantees a strong surface–surface stabilizing hydration repulsion [43]. On the other hand, the cost in free energy (energy minus orientation entropy) needed to disrupt the water network near passive surfaces leads to a depletion of H_2O molecules (dewetting of the surface) and to a surface-surface hydrophobic attraction. The effect is amplified if the surfaces carry hydrophobic groups (hydrocarbons, fluorocarbons, ...). The hydration force has been measured in numerous osmotic pressure [58] or SFA experiments [9]. The data are usually adjusted with an exponentially decreasing function of the surface–surface separation, the characteristic distance being of the order of 1–10 Å. From the theoretical point of view, refined discrete models of water fluids have been studied in bulk or near various surfaces [59–61]. The different density profiles vary rapidly on fractions of ångstroms due to the complex, non-spherical nature of the direct potentials. The resulting force between surfaces presents a rich structure which strongly depends on the details of the coulombic interaction parameters. In particular, the hydration force and the associated stability seems to be very sensitive to the presence of ions and may vary drastically when 'specific' ion–solvent and ion–surface interactions are introduced [62]. The debate about the quantitative explanation of the measured hydration force and about the precise role of the water anisotropy on the apparent exponential behaviour is still open [57, 63].

4. Colloidal interactions in charged systems

We now focus on solutions of charged colloids and small ions. Within the so-called Primitive Model (PM), the discrete nature of the polar solvent is forgotten and mixtures of charged hard spheres (diameter σ_i, charge valence Z_i, concentration ρ_i) immersed in a continuous solvent of dielectric constant ε are considered [19]. The PM pair potentials (solvent-averaged potentials of mean force) are

$$\begin{aligned}
\beta v_{ij}(r) &= +\infty && r < \sigma_{ij} \\
&= Z_i Z_j L_B / r && r > \sigma_{ij}
\end{aligned} \tag{33}$$

where the Bjerrum length $L_B = e^2/(4\pi\varepsilon_0\varepsilon kT)$ is the single parameter which takes the solvent implicitly into account. $L_B \approx 7$ Å in aqueous solutions at room temperature. It is implicitly assumed in (33) that the interior of the charged particles has the same dielectric constant than the solvent (no electrostatic images).

In such mixtures viewed as asymmetrical electrolytes, the colloidal spheres c are much larger and more highly charged than the simple ions. Despite its crude, 'primitive'-treatment of the solvent (neglect of van der Waals and hydration forces), the PM contains most of the characteristics of charged systems: (i) the infinite range of the $1/r$ coulombic potentials, (ii) the simultaneous presence of positive and negative charges in order to guarantee the electroneutrality condition $\sum \rho_i Z_i = 0$, (iii) the coupling between ++, −− repulsions and +− attractions. As before, the aim is to find out the effective, *ion-averaged* potential of mean force between colloids, in a description where the small ions play the role of the solvent in the general analysis. In contrast to what happened in neutral systems, the treatment in terms of virial expansion is now useless because of the points (i)–(iii) and special approaches are required.

Since the 1910s, the problem of charged systems has been attacked from different directions, at different levels of approximation. The concept of electrostatic screening introduced by Gouy, Chapman and Hückel in the 1910–20s, led to the famous DLVO screened coulombic, effective potential between colloids in the 1940s [64]. Since the 1960s, numerous studies of the Poisson–Boltzmann (PB) approach have derived the notion of ionic condensation and effective colloidal charge, reminiscent of the Bjerrum concept of ionic association in the 1920s. The approach based on the numerical resolution of integral equations (especially HNC-like closures) was developed for the PM of colloids in the early 1980s.

Concerning the 'exact', reference treatment based on numerical Monte Carlo (MC) or molecular dynamics (MD) simulation, which could serve as tests of the validity of approximate theories, only a few studies of bulk charged colloidal systems, with size and charge asymmetry in the salt-free micellar regime, have been performed since the early 1980s [65–69]. The relative lack of PM simulation data illustrates the technical difficulties related to the three points described above: (i) the long-range nature of the potentials implies the heavy, time-consuming calculation of Ewald sums at each colloid-ion configuration, (ii) the total number of particles rapidly becomes large as the charge asymmetry increases since even a reasonable number of colloids must be accompanied by a large number of counter-ions in order to maintain the electroneutrality of the system and (iii) last but not least, the accumulation of counter-ions in the vicinity of the colloidal surfaces implies the use of very small MC displacements or short MD time steps in order to avoid colloid–counter-ion overlaps and thus an astronomic number of steps to get a good statistic in the correlations (investigation of colloid–ion cluster moves seems to be a good direction to follow in order to overcome this last difficulty [70]). These reasons explain why only charge asymmetries of $1/-10$ to $2/-20$ have been published in the literature in the last 20 years [65–67, 69] and why, as a consequence, unusual behaviours derived by approximate theories at higher charge cannot be validated without ambiguity. Although very recent publications support some optimism [68–71], one must admit that, even half a century after DLVO, bulk colloidal systems are still not yet 'exactly' understood at high electrostatic coupling, quantitatively as well as qualitatively.

While PM simulation is difficult in bulk, it becomes easier and has been intensively used since the early 1980s in the fundamental, special case of two parallel, charged walls separated by a simple electrolyte [72]. In that case, there are only two fixed colloidal surfaces (two interacting double layers) and the previous difficulties disappear. The data are analysed in pressure versus wall–wall separation curves. Thank to these complete simulation studies, one could say that the behaviour of this particular geometry is exactly known since the 1980s.

In the last few years, one observes in the literature a return to the problem of charged colloidal systems. Recent analyses based on modern theories like the density functional theory (DFT) have brought fruitful points of view. They have also led to a few controversies, especially about the fascinating issue of effective, purely electrostatic attraction between like-charged colloids.

The purpose of this section is (i) to recall the correct equilibrium and structural properties of the PM through well established but sometimes mis-appreciated approaches; (ii) to clarify the controversies and discuss the new analyses in view of the traditional theories and (iii) to describe the traps to avoid in the understanding of salt-free colloidal systems and criticize statements which violate subtle but fundamental notions of electrostatics. For such purpose, I have to begin at the trivial but sometimes forgotten bulk Debye–Hückel (DH) level. The specialists could skip this introduction.

In the following, we will investigate cationic colloids ($Z_c > 0$) of density ρ_c and monovalent counter-ions $Z_- = -1$ mixed with the monovalent $+1/-1$ salt of same counter-

ion. Generalization to mixed valences is straightforward. If ρ_s and ρ_s' represent the salt concentration inside the solution and the salt reservoir, respectively, the ionic concentrations in the three component system are imposed by the electroneutrality condition:

$$\rho_- = Z_c \rho_c + \rho_s$$
$$\rho_+ = \rho_s$$

while $\rho_-' = \rho_+' = \rho_s'$ in the reservoir. Ions can cross the semi-permeable membrane only by neutral pairs. The salinity in the solution is identified with the co-ion concentration. It is in general lower than the salinity imposed in the reservoir due to the Donnan, salt exclusion effect. The equilibrium condition which sets the value of ρ_s is the equality of the chemical potential of salt in both compartments:

$$\mu_s = \mu_+ + \mu_- = \mu_s' = \mu_+' + \mu_-'. \tag{34}$$

The net osmotic pressure Π of the solution (against the electrolyte reservoir) is the difference between the pressures of the solution P and of the reservoir P' (within the PM, P and P' represent the pressures of the gas of charged particles; experimentally, there are themselves osmotic pressures against *pure* water). The thermodynamic derivative (14) becomes

$$\chi_{osm} = \left(\frac{\partial \rho_c}{\partial \beta \Pi} \right)_{\rho_s'} = S_{cc}(0). \tag{35}$$

In the important salt-free case, $\rho_s = \rho_s' = 0$, the two-component system colloid + counter-ion verifies the local electroneutrality conditions:

$$\frac{Z_c}{Z_c + 1} \chi = S_{--}(0) = \sqrt{Z_c} S_{c-}(0) = Z_c S_{cc}(0). \tag{36}$$

4.1. Debye–Hückel theory

In principle, the DH approximation gives the exact asymptotic (infinite dilution) law. Although its domain of validity for colloids is in practice restricted to unrealistically high dilutions, its analysis is useful to illustrate some fundamental concepts.

Within the bare DH approximation, all charged species, ions as well as colloids, are considered as pointlike ions ($\sigma_i = 0$) and the correlations are treated at a linearized mean-field level. Inserting the MSA direct correlation functions, $c_{ij}(r) = -Z_i Z_j L_B / r$, $r > 0$, in the PM–OZ equation (12) yields for the total correlations

$$g_{ij}(r) = 1 - \frac{Z_i Z_j L_B}{r} e^{-\kappa_0 r} \tag{37}$$

where the total screening constant κ_0 involves the contribution of the ions *and* the colloids:

$$\kappa_0 = \sqrt{4\pi L_B [2\rho_s + Z_c(Z_c + 1)\rho_c]}. \tag{38}$$

The PM virial (9) and compressibility (10) routes give different expressions for the pressure of the solution:

$$\beta P_c = \rho = 2\rho_s + (Z_c + 1)\rho_c \tag{39}$$

$$\beta P_v = \rho - \frac{\kappa_0^3}{24\pi}. \tag{40}$$

This thermodynamic inconsistency illustrates the approximate nature of the DH theory. While the compressibility pressure (39) is reduced to the perfect gas law, the virial route (40) is richer since it exhibits the first non-ideality correction in the equation of state. This behaviour is common to all DH-like theories. Note that the extra term in (40) is negative and could induce,

in principle, a van der Waals loop in isotherm $P(\rho)$ curves and a liquid–gas phase transition in the phase diagram [73]. In fact, this would happen in concentration–charge regimes where the bare DH equation of state (40) breaks down. For symmetrical electrolytes (restricted PM), more analytical terms could be added to give reasonable predictions [74] compared to exact MC phase diagrams [75]. For colloidal systems, this direction is less powerful [28].

Corresponding expressions are obtained for the pressure P' in the reservoir. Using the compressibility route, the net osmotic pressure is given by

$$\beta\Pi = \rho_c(1 + Z_c) + 2(\rho_s - \rho'_s). \tag{41}$$

The relation between the values of salinity in the two compartments is

$$\rho_s(\rho_s + Z_c\rho_c) = \rho'^2_s. \tag{42}$$

This means that the DH ionic chemical potentials μ_i are identified with their ideal expressions $kT \ln \rho_i$ (again within the compressibility route). Note that the resulting expression (41) for Π could be directly obtained from the osmotic derivative (35).

Two important limited cases can be investigated. In excess of salt or at low colloidal concentration (namely, $Z_c\rho_c \ll \rho'_s$):

$$\rho_s \approx \rho'_s - \frac{Z_c\rho_c}{2}$$

$$\beta\Pi \approx \rho_c + \frac{Z^2_c\rho^2_c}{4\rho'_s}. \tag{43}$$

This means that when one colloid with its Z_c counter-ions is inserted inside the solution, $Z_c/2$ pairs of salt ions leave the solution through the membrane. The net pressure is increased by only one kT/V. On the other hand, for salt-free cases ($Z_c\rho_c \gg \rho'_s$), the salinity inside the solution is negligibly small ($\rho_s \ll \rho'_s$) and all counter-ions contribute to the perfect gas pressure:

$$\beta\Pi = \rho_c(1 + Z_c). \tag{44}$$

According to (37), the *cc* pair potential of mean force $\beta w_{cc} = -\ln(g_{cc}) \approx 1 - g_{cc}$ takes the screened coulombic, repulsive form

$$\beta w_{cc}(r) = \frac{Z^2_c L_B}{r} \, e^{-\kappa_0 r}. \tag{45}$$

On the other hand, the *cc* effective pair potential v^{eff}_{cc} extracted from the OCM–OZ equation (26) coupled with the MSA closure reads

$$\beta v^{eff}_{cc}(r) = \frac{Z^2_c L_B}{r} \, e^{-\kappa r} \tag{46}$$

where the screening constant κ now involves only the *ionic* contributions:

$$\kappa = \sqrt{4\pi L_B[2\rho_s + Z_c\rho_c]}. \tag{47}$$

The fundamental difference in nature between these two potentials is illustrated in (45) and (46). The colloids contribute to the electrostatic screening ($\kappa^2_0 = \kappa^2 + \kappa^2_c$ with $\kappa^2_c = 4\pi L_B\rho_c Z^2_c$) only in the ion + colloid-averaged potential w_{cc} and not in the ion-averaged potential v^{eff}_{cc}. In the presence of salt, the two quantities coincide at zero colloidal concentration, the ionic strength being dominated by the salt ions. This case follows the general behaviour described for neutral systems. In the opposite (and more exciting), salt-free limit, κ contains only the counter-ion contribution and, due to the electroneutrality condition, v^{eff}_{cc} becomes ρ_c-dependent and is $(1 + Z_c)^{1/2}$ less screened than w_{cc}. This behaviour remains valid even at high or infinite

dilution of the colloids (in the mathematical sense that two potentials of different screening differ even when both screening tend to zero). From this point of view, salt-free colloidal solutions can *never* be considered as dilute. As ρ_c decreases, the ionic screening decreases in parallel ($\approx(\rho_c Z_c)^{1/2}$) and the colloids remain coupled at larger distances.

For salt-free systems, it is important to emphasize the mistake which consists in using without caution the OCM limiting law $g_{cc} = \exp(-\beta v_{cc}^{eff})$ at zero density and thus identifying w_{cc} with v_{cc}^{eff}. This would lead to the obviously wrong result $\chi_{osm} = S_{cc}(0) = 1 - Z_c$. This limiting law is valid in general *except* for the present salt-free case. The correct reasoning uses the limiting law $c_{cc}^{eff} = -\beta v_{cc}^{eff}$, which remains valid in all circumstances and which leads, through the OCM–OZ equation, to expression (37) for g_{cc} and to the correct, perfect gas law $\chi_{osm} = 1/(1 + Z_c)$. Ignoring these subtleties and confusing effective and mean-force potentials could lead to severe misinterpretations [76].

It is interesting to verify that the OCM compressibility route is able to exhibit the perfect gas pressure of the counter-ions despite the non-explicit treatment of their degrees of freedom. This illustrates the electroneutrality condition hidden behind the DH expression for g_{cc}. On the other hand, as noted in the general analysis, the OCM virial route is not so valid. Indeed, introducing the effective potential (46) in the OCM virial equation (2) gives for the leading term (no salt, $\rho_c \to 0$) $\beta\Pi \approx \rho_c(1 + Z_c/2)$!

Before closing this section on the basic DH approach, we return to the electrostatic depletion versus screening discussion in complex charged colloidal mixtures, already mentioned in 3.2–3.3. The large colloids are now surrounded by ions (of screening constant κ) as well as small 'solvent' colloids or polymer impurities (κ_s). Starting from the PM describing all species with coulombic potentials or from the intermediate model describing large and small colloids only with ion-averaged screened coulombic potentials, the effective interaction between large colloids averaged over all remaining components reads within the DH approximation

$$\beta v_{cc}^{eff}(r) = \frac{Z_c^2 L_B}{r} \exp[-(\kappa^2 + \kappa_s^2)^{1/2} r]. \tag{48}$$

At this DH level of description, the small colloids are considered as pointlike multivalent ions, only contributing to the total ionic strength. When the density of this component is low, the total screening factor may be expanded. Keeping the first order in ρ_s only, the effective potential becomes

$$\beta v_{cc}^{eff}(r) \underset{small\ \rho_s}{\approx} \frac{Z_c^2 L_B}{r} e^{-\kappa r} \left(1 - \frac{\kappa_s^2}{2\kappa} r\right). \tag{49}$$

The negative contribution in the right-hand side of (49) is nothing else than the leading term (27) in the virial diagrammatic expansion applied to the intermediate model (with linearization of the *cs* correlations). Use of (49) without caution would lead to the incorrect conclusion that the depletion attraction of electrostatic origin due to the solvent colloids dominates at large distances, in contradiction with the pure repulsion in the original expression (48). The importance of higher order terms in the expansion (the so-called ring diagrams [1]) illustrates again the long-range and multi-body character of the electrostatic screening. A true depletion attraction in charged mixtures may exist only beyond the DH linearized treatment of the *cs* correlations [49].

4.2. Improved DH-like theories

The main failure of the bare DH theory is the neglect of the colloidal size and the linearized treatment of the *cc* correlations. As a direct consequence, $g_{cc}(r)$ presents non-physical

negative values at short distances. Introducing a finite value for $\sigma_c = 2a$ and replacing the cc MSA closure by a more adapted, nonlinearized, approach (HNC integral equation) does not qualitatively change the final DH results. Numerous analyses successfully followed this direction in the early 1980s and derived important, somewhat forgotten, conclusions. As a first step, we leave the cc MSA treatment, still neglecting the colloidal size. The present derivation is very similar in spirit to the pioneer study by Beresford-Smith *et al* [20]. The MSA–DH c_{ci} and c_{ij} ($i, j =$ ions) are inserted in the PM–OZ equation (12) while no assumption is made on g_{cc}. Mapping the PM into the effective OCM (26) allows us to derive the same bare DH v_{cc}^{eff} (46) as before (inclusion of cc bridge functions beyond the HNC closure would affect this effective potential at short distances). In parallel, g_{ci} and g_{ij} can be expressed as convolution products of g_{cc} and v_{cc}^{eff}. Introducing these functions in the PM virial equation (9) leads to the pressure

$$\beta P = \rho - \frac{\kappa(\kappa^2 + \frac{3}{2}\kappa_c^2)}{24\pi} + \frac{\rho_c \kappa_c^2}{24\pi} \int_0^\infty g_{cc}(r) \left(1 - \frac{\kappa r}{2}\right) \frac{e^{-\kappa r}}{r} \, dr \qquad (50)$$

Note that g_{cc} could be replaced by h_{cc} without modifying the integral in (50). The DH virial equation of state (40) could be recovered by inserting (37) in (50). The equation of state (50) contains three terms: the perfect gas pressure of all particles, a negative contribution which is independent of the colloidal positions and an integral term which depends on the cc correlations. In the absence of salt, (50) becomes

$$\beta \Pi = \beta P = \rho_c(1 + Z_c) - \frac{\kappa^3(1 + \frac{3}{2}Z_c)}{24\pi} + \frac{\rho_c \kappa_c^2}{24\pi} \int_0^\infty g_{cc}(r) \left(1 - \frac{\kappa r}{2}\right) \frac{e^{-\kappa r}}{r} \, dr. \qquad (51)$$

Using without caution the OCM virial equation (2) with the effective potential (46) leads to (no salt)

$$\beta P = \rho_c \left(1 + \frac{Z_c}{2}\right) + \frac{\rho_c \kappa_c^2}{24\pi} \int_0^\infty h_{cc}(r)(1 + \kappa r) \frac{e^{-\kappa r}}{r} \, dr. \qquad (52)$$

The already mentioned factor $\frac{1}{2}$ in the counter-ionic perfect gas pressure is inadequate. One must keep in mind that the OCM virial equation (2) was established for a density-independent pair potential $v(r)$. Generalization to ρ-dependent $v(r)$ consists in formally replacing $v'(r)r/3$ by $v'(r)r/3 - \partial v(r)/\partial \ln \rho$ in (2). For the present screened coulombic potential, the modified OCM virial equation becomes (no salt)

$$\beta P = \rho_c + \frac{\rho_c \kappa_c^2}{24\pi} \int_0^\infty g_{cc}(r) \left(1 - \frac{\kappa r}{2}\right) \frac{e^{-\kappa r}}{r} \, dr. \qquad (53)$$

Now, the perfect gas pressure of the counter-ions has completely disappeared. On the other hand, the integrals in (53) and (51) coincide. The extra terms in the PM virial equation which are not captured by the OCM virial approach illustrate the importance for the thermodynamics of zero- and one-body terms in the full potential of mean force. For a discussion at the free energy level, see [20]. A similar DH analysis has been recently proposed in [77].

If the finite colloidal size is taken into account, the previous approach remains analytical and the DH-like conclusions remain valid (although the final expressions become much heavier):

(i) v_{cc}^{eff} keeps its screened coulombic, repulsive form (MSA or HNC closure for the cc correlations) [26–29, 78]:

$$\beta v_{cc}^{eff}(r) = Z_c^2 L_B X^2 \frac{e^{-\kappa r}}{r} \qquad r > 2a. \qquad (54)$$

Note again that the equality in (54) is restricted to the large separation regime when *cc* bridge functions are introduced.

The factor X is a function of κa and of the *cc* correlations [29]:

$$X = \frac{e^{\kappa a}}{1 + \kappa a + e^{-\kappa a}(\sinh \kappa a - \kappa a \cosh \kappa a)\rho_c \int_0^\infty dr \, g_{cc}(r) \, e^{-\kappa(r-2a)}/\kappa r}. \tag{55}$$

When the last term in the denominator of (55) is discarded (which is valid at low volume fraction), the resulting effective potential takes the famous DLVO form [64], originally deduced from the linearized Poisson–Boltzmann approach (see 4.3) [26, 27, 78]:

$$\beta v_{cc}^{eff}(r) = \frac{Z_c^2 L_B}{(1 + \kappa a)^2} \frac{e^{-\kappa(r-2a)}}{r} \qquad r > 2a. \tag{56}$$

Due to the minimum contact distance a, the ions are rejected farther from the colloid centre, their screening ability is weaker and the *cc* repulsion is stronger. At higher colloidal density, the integral term in (55) is non-negligible and the ρ_c-dependent pair potential between two colloids is perturbed by the presence of colloidal neighbours [26–29]. This illustrates how the effective pair potential takes many-body correlations into account.

(ii) Since v_{cc}^{eff} remains repulsive, this means that the osmotic compressibility χ_{osm} derived from the compressibility equation is finite (and low) and the corresponding equation of state is monotonic without special features.

(iii) On the other hand, the PM virial equation of state exhibits a negative electrostatic contribution similar to the $-\kappa^3$ term in (40) or in (50) [79], which may induce van der Waals loops and a liquid–gas phase transition. The simultaneous presence at the same thermodynamic state of a diverging virial compressibility and of a purely repulsive effective potential again illustrates the approximate nature and thermodynamic inconsistency of DH-like treatments (only comparisons with more refined theories or exact simulation data could say which DH route is the most accurate one for a given state). In a correct approach, compressibility and virial PM osmotic pressures must coincide; if a PM spinodal line is approached as near a critical point, the divergence of χ_{osm} implies high values of $S_{cc}(q)$ at zero angle according to (35) and thus long-range positive correlations in $g_{cc}(r)$. Since by definition these functions are identical within the effective OCM and the PM, the effective pair potential associated with the OCM must present attractive values in this region of the phase diagram (note that nothing can be concluded *a priori* about the sign of the effective interaction *far* from the spinodal line).

The next step in an improved theory involves a treatment of the colloid–ion correlations at a nonlinearized level. Using the integral equation approach, this can be done by replacing the MSA with the HNC closure [80]. A similar but not fully equivalent approximation is based on the Poisson–Boltzmann equation, which will be described first.

4.3. Poisson–Boltzmann theory

The objective of this approach is to calculate the local average ionic densities $\rho_i(r)$ and the local average electrostatic potential $\psi(r)$ around the colloids fixed in the configuration (r^{N_c}). The inhomogeneous ionic fluid is in osmotic equilibrium with the salt reservoir and feels external forces of excluded volume and electrostatic origin exerted by the macro-ions. The exact Poisson equation relates ψ or the electric field $E = -\nabla\psi$ to the average charge density ρ_{el}:

$$\Delta \varepsilon \psi = -\text{div} \, \varepsilon E = -\rho_{el}/\varepsilon_0 = -e(Z_c \rho_c + \sum_i Z_i \rho_i)/\varepsilon_0. \tag{57}$$

Dielectric discontinuities at the colloidal surfaces, $|r - r_c| = a$, can be taken into account in (57).

Within the Poisson–Boltzmann (PB) approximation, all ions are assumed to be pointlike and the N_c-body potential of mean force (semi-grand potential of the inhomogeneous fluid) is expressed as [22, 64, 81, 82]:

$$W_{N_c}(r^{N_c}) = U - TS - \sum_i \mu_i N_i$$

$$U = \frac{1}{2} \int \rho_{el}(r)\psi(r)\,dr = \frac{1}{2} \int \varepsilon_0 \varepsilon E^2(r)\,dr$$

$$-TS = kT \sum_i \int \rho_i(r)(\ln \rho_i(r) - 1)\,dr$$

$$\mu_i N_i = \mu_i' N_i = kT \ln \rho_i' \int \rho_i(r)\,dr. \tag{58}$$

The integral in the electrostatic energy U is over the fluid volume as well as the interior of the colloids. The integral in the entropy S is over the fluid volume only. The last equation identifies the ionic chemical potentials in the solution with their values in the reservoir and guarantees the osmotic equilibrium. The zero of potential ψ is arbitrarily chosen in the reservoir. Expressions (58) are valid for fixed colloidal charge (constant charge boundary condition) and must be completed by extra terms [81] if instead the surface potential is fixed (constant potential) or if the charging process of the surfaces results from chemical equilibrium between surface sites and bulk ions (charge regulation [83]). The ionic profiles are given by the mean-field Boltzmann approximation:

$$\rho_i(r) = \rho_i' \exp[-Z_i e\psi(r)/kT] = \rho_i' \exp[-Z_i \varphi(r)] \qquad r \in \text{fluid} \tag{59}$$

where $\varphi = e\psi/kT = \psi/25$ mV.

This law can be elegantly recovered within the density functional theory (DFT) formalism [84] by considering W_{N_c} in (58) as a *functional* of the colloidal densities and by using the equilibrium condition $\delta W_{N_c}/\delta \rho_i = 0$ (*functional* derivative).

Insertion of these ionic profiles in the Poisson equation leads to the PB equation which, for $+1/-1$ reservoir electrolyte, takes the well known form

$$\Delta\varphi = \kappa'^2 \sinh\varphi \qquad r \in \text{fluid} \tag{60}$$

while the Laplace equation $\Delta\varphi = 0$ holds inside the particles. $\kappa' = 8\pi L_B \rho_s'$ represents the screening constant inside the reservoir. Again, the PB equation (60) implicitly guarantees that the salt chemical potential $\mu_s = \mu_+ + \mu_- = 2kT \ln \rho_s'$ is uniform everywhere in the ionic fluid and in the reservoir. The constant charge boundary condition relates the external and internal normal electric fields at the colloidal surfaces to the surface charge density $\Sigma_c = Z_c/(4\pi a^2)$:

$$\nabla_n \varphi_{ext} - \varepsilon_{int}/\varepsilon \nabla_n \varphi_{int} = -4\pi L_B \Sigma_c. \tag{61}$$

This condition automatically expresses the global electroneutrality of the solution.

The salinity ρ_s inside the solution is obtained by averaging the co-ion profile. In experiments performed without osmotic exchange, it is this quantity rather than ρ_s' which is fixed and known. In that case, ρ_s' is formally considered as a parameter *a posteriori* adjusted to give the correct ionic content in the solution. The salt-free limit is continuously reached by simply investigating, in the scheme above, very low values of ρ_s' or κ'. As $\rho_s' \to 0$, φ is shifted by the additive constant $-\ln \rho_s'$, the co-ion profile vanishes ($\sinh\varphi$ and $\cosh\varphi$ may be replaced by $\exp(\varphi)/2$) and the precise value of ρ_s' becomes irrelevant for the counter-ion profile.

In a linearized version, φ is supposed to take low values (the local densities are close to ρ_s'), $\sinh \varphi$ is expanded to first order in φ and the PB equation is replaced by the linearized PB or DH equation:

$$\Delta \varphi = \kappa'^2 \varphi \qquad r \in \text{fluid.} \tag{62}$$

This corresponds to expanding the *functional S* up to second order in the ionic profiles ρ_i [84]. While the nonlinearized PB equation is adapted to all salinity, (62) is restricted to salt excess ($Z_c \rho_c \ll \rho_s'$). At low added salinity or in the absence of salt, the expansion must be performed to first order in $\varphi - \varphi_0$ rather than φ where φ_0 is the potential somewhere to be chosen inside the solution. The resulting linear equation contains φ_0-dependent screening and constant terms and loses its general character.

The implicit approximations assumed by the PB theory are of mean-field nature. The average of the product of the instantaneous charge density and electrostatic potential has been replaced in U by the product of the averages of these quantities, $\rho_{el}\psi$ (this would correspond to replacing the two-particle density $\rho_{ss}(r, r')$ by the product $\rho_s(r)\rho_s(r')$ in the general virial equation (18), neglecting the inhomogeneous $h_{ss}(r, r')$ function [20]). The entropy S of the ionic fluid has been replaced by its ideal expression. Equivalently, the local ionic profiles $\rho_i(r)$ which are expressed in an exact theory as N-body statistical averages of the microscopic Boltzmann factor $\exp(-\beta U_N)$ are replaced here by the exponential of the mean interaction, $\exp(-\beta Z_i e \psi)$. In other words, the ionic fluctuations or ion–ion correlations are neglected in the PB mean-field theory.

The main task is to solve the PB equation (60) with the boundary condition (61) (or an equivalent one). For a general colloid configuration, this requires a formidable numerical calculation [22], even in the linearized version. The PB equation is a second-order differential equation with partial derivatives. The fluid boundary at the colloidal surfaces where the condition (61) applies is a complex surface in the three-dimensional solution. 'Reflections' of the electrostatic potential coming from one colloid onto the hard-sphere neighbours or 'overlaps' of the ionic layers around all colloids induce in general a complex, N_c-body map of φ, which cannot be decomposed as a sum of one-body contributions. Nowhere in the solution are φ and its gradient simultaneously known *a priori* Thus, a numerical calculation starts with a guess for $\varphi(r)$ and follows iterative procedures using Newton–Raphson techniques and up-to-date numerical analysis to speed up the convergence [85].

Once the local potential $\varphi(r)$ and ionic densities $\rho_i(r)$ are obtained, many important quantities relative to the colloids and to the thermodynamics can be deduced. The force acting on colloid c is [81]

$$\boldsymbol{F}_c = -\nabla_c W_{N_c} = \int_c \mathbf{T} \, \mathrm{d}\boldsymbol{S}. \tag{63}$$

By convention, the vector $\mathrm{d}\boldsymbol{S}$ points towards the ionic fluid. The tensor $\mathbf{T}$ contains an electrostatic part $\mathbf{T}_{el}$ and a kinetic or thermal part $\mathbf{T}_{th}$:

$$\mathbf{T} = \mathbf{T}_{el} + T_{th} = \varepsilon_0 \varepsilon (\boldsymbol{EE} - \tfrac{1}{2} E^2 \mathbf{I}) - kT \rho_{ion} \boldsymbol{I}. \tag{64}$$

$\mathbf{T}_{el}$ is the Maxwell tensor, which gives the electric force exerted on a charged surface (excluding the self electric field due to the surface itself). $\mathbf{T}_{th}$ represents the perfect gas osmotic pressure due to all ions of local total density ρ_{ion}. Since the tensor $\mathbf{T}$ is divergence free ($\mathrm{div}\, \mathbf{T} = 0$), the surface integral in (63) can be performed on the surface of colloid c as well as on any larger closed surface surrounding the previous one and excluding colloidal neighbours. Physically, this expresses the fact that each elementary ionic volume is at equilibrium, the electric force being exactly balanced by the ion osmotic pressure gradient (thermal force). This freedom in the choice of integration surface can be advantageously used to minimize numerical errors in

the force calculation. Indeed, the electric and thermal parts are high and opposite in sign near the macro-ions and must be determined very accurately in order to extract the small difference with a reasonable precision. It is thus preferable to choose a closed surface located farther from the macro-ion, at mid-distance with the first neighbours, where the full tensor is dominated by the thermal part. Additionally, this optimal choice allows us to deduce in some simple geometry the sign of the force before any numerical calculation (see below).

Following the same route, the pressure $P = -\delta W_{N_c}/\delta V$ can be obtained by investigating a small increase δV of the volume V. In that case, the frontier of the solution (cell edge) as well as the position of the N_c colloids are homothetically rescaled by the relative value $\delta_r/r = \delta V/3V$. The resulting increase in W_{N_c} gives [81]

$$P = \rho_c kT + \frac{1}{3V}\left\langle \sum_{\text{col}} \boldsymbol{r}_c \boldsymbol{F}_c \right\rangle_c - \frac{1}{3V}\left\langle \int_{\text{cell}} \boldsymbol{r}\rho_{ion} kT \, \mathrm{d}\boldsymbol{S} \right\rangle_c. \tag{65}$$

The same expression can be elegantly recovered from the PM virial equation (18) by noting that the electric force $Z_i e\boldsymbol{E}$ applied on ion i is equal to the osmotic force $kT\nabla\ln\rho_i$ within the PB approximation. The equation of state contains three terms, the perfect gas pressure of the colloids, the colloid–colloid correlation term and the ionic contribution, which depends on the local ionic density at the cell edge. If this density is uniform, the ions contribute as $\rho_{\text{cell}} kT$ to P [86, 87]. Note again that the OCM virial equation (19) would miss this last contribution. Lastly, the osmotic pressure Π is obtained by subtracting the reservoir pressure $P' = 2\rho'_s kT$ from P.

We now apply these general PB expressions to specific configurations, starting from the simplest case of one isolated colloid immersed in an electrolyte ($N_c = 1$, $\rho'_s \neq 0$). On the analogy of the linearized, DH solution, the long distance behaviour of the PB solution (60) is written as [88] (r is measured from the centre of the colloid):

$$\varphi(r) \underset{\kappa(r-a)\gg 1}{\approx} \frac{Z_c^{eff} L_B}{(1+\kappa a)}\frac{e^{-\kappa(r-a)}}{r}. \tag{66}$$

The powerful concept of effective charge Z_c^{eff} or charge renormalization is very general [89] and illustrates the strong accumulation or ionic *condensation* of counter-ions in the vicinity of colloid surfaces. Because of this short-range, non-linear effect, the colloid can be regarded far from its surface as if, at the linearized, DH level, it carried a weaker, partially neutralized charge, $Z_c^{eff} < Z_c$, which depends on Z_c and κa. Within the PB approximation, Z_c^{eff} saturates to a constant value as the colloid becomes highly charged. In that regime, an increase of Z_c is counterbalanced by an equal increase in the condensed charge and the long-range potential becomes independent of the details on the colloidal surface. More details on the ionic condensation around spheres could be found in a recent review [90].

For two interacting colloids separated by the centre-to-centre distance D in an electrolyte [91], the PB force is *a priori* always *repulsive*. Indeed, integrating the stress tensor on the closed surface constituted by the mid-plane between the colloids, where $\boldsymbol{E}\,\mathrm{d}\boldsymbol{S} = 0$ by symmetry, and a hemisphere of infinite radius, where $E = 0$ and $\rho_{ion} = 2\rho'_s$, leads to the expression

$$F_c = \iint_{\text{mid-plane}} \left(\frac{\varepsilon_0\varepsilon}{2}E^2 + (\rho_{ion} - 2\rho'_s)kT\right)\mathrm{d}S \tag{67}$$

which is obviously positive.

The configuration of two colloids has been extensively studied since the DLVO pioneer works. For large colloids near contact ($\kappa'a \gg 1$, $D - 2a \ll a$), it is sufficient to study the simpler, one-dimensional geometry of two parallel charged plates (of same charge density than the colloids) and use the Derjaguin approximation to deduce the colloid–colloid force. For

a general configuration, the PB equation requires a more complex resolution. The potential $\varphi(r, \theta)$ depends on the distance r to one colloid and on the angle θ between r and the axis joining the colloids. In the linearized DH version, φ can be analytically expressed as an infinite expansion in Bessel functions in r and Legendre polynomials in $\cos \theta$ [64, 92]. In the nonlinearized PB case, bispherical coordinates are adapted to the numerical resolution [93]. Note that the complete and systematic numerical PB solution was obtained only in the early 1990s (and for moderate surface charge), 40 years after the first studies. This illustrates the difficulty of the numerical problem, even for this fundamental and apparently simple geometry.

An analytical expression for the force or the effective, mean-force pair potential can be derived in the asymptotic regime of large separations, $\kappa(D - 2a) \gg 1$. The weak overlap or linear superposition approximation applies and the potential far from the two particles, in particular at the mid-plane, is the sum of the contributions due to each colloid, taken as isolated. Inserting the long-range expression (66) for each contribution in (67) gives for the pair interaction

$$\beta v_{cc}^{eff}(r) = \frac{Z_c^{eff^2} L_B}{(1 + \kappa a)^2} \frac{e^{-\kappa(r-2a)}}{r} \qquad \kappa(2 - 2a) \gg 1. \tag{68}$$

In the linearized case, Z_c^{eff} is replaced by the bare value Z_c and the famous DLVO potential (56), already mentioned, is recovered. One must keep in mind that this expression is in principle valid only at large separations. At shorter distances, the weak-overlap approximation and the identification (66) break down, and departures from the asymptotic screened coulombic force are observed, *even* in the linearized version [92].

The DLVO potential (56), (68) has been the starting point of thousands of studies and has allowed a qualitative as well as quantitative understanding of the following phenomena: (i) the stability of charged dispersions against irreversible aggregation [64]; (ii) the short-range liquid order observed in scattering [2–6]; (iii) the fluid–crystal transition which appears at low ionic strength [94]; (iv) the direct pair force measurements [9–16]; (v) the PM simulation data [67]; .... The effective charge is usually considered as an adjustable parameter or is chosen according to *a priori* theoretical predictions [88–90].

The PB resolution becomes very difficult in more complex geometries involving numerous colloids (see the beautiful example in [22]). As far as the ionic profiles around macro-ions in concentrated solutions are concerned, a simple alternative is to use the cell geometry. The solution is divided into N_c spherical, overall neutral cells, each containing one centred colloid. The cell radius R is related to the colloidal concentration, $\rho_c 4\pi/3R^3 = 1$. The spherically symmetric PB equation is easily solved from $r = a$ to $r = R$ (where $E = 0$). The counter-ion profiles are used to deduce effective charge values as a function of colloidal density, even in the absence of salt [90]. According to (65), the PB osmotic pressure is given by the edge ionic density [86], $\Pi = (\rho_{ion}(R) - 2\rho_s')kT$, and successfully reproduces experimental equations of state [5]. Of course, this simple cell geometry is not adapted to derive colloidal forces since $F_c = 0$ by symmetry. Investigating eccentric positions of the macro-ion in the cell or the presence of two colloids in the same cell seems to be a good direction to follow to get further insights into the colloidal interactions at finite density [95].

Another geometry consists of two colloids confined near a planar wall or between two parallel walls or inside a cylindrical pore. The two particles are at the same distance from the wall. An elegant analytical proof has recently generalized the bulk result [96]: the force felt by each colloid, projected along the wall, is always repulsive, whatever the charge state, boundary condition and dielectric property of the walls and the colloids. This *a posteriori* invalidates numerical PB data which predicted attraction between particles [97] and indicates that experimental evidences of such attraction [15, 16, 98] must be interpreted with different

approaches.

In the last few years, the PB approach has been revisited in terms of the density functional theory [82, 84, 99]. Instead of solving directly the PB equation, this new formulation focuses on the strictly equivalent free-energy functional (58). Making the same kind of approximations as in older PB or integral equation analyses (linearization, weak overlap approximations), it becomes possible to recover in an elegant way the DLVO pair potential between particles as well as the negative, DH-like, one-body term in the equation of state or free energy [100]. Attempts have been made to go beyond this level of approximation and to introduce partial nonlinear and multi-body corrections. The resulting expressions for the colloidal forces remain tractable but must be used with caution since their domain of validity is not always well controlled. As an illuminating example of its limitation, such analysis has recently predicted an attraction between confined particles [101], in violation of the exact PB behaviour [96]. It is clear that such analytical treatments are adapted to give the asymptotic, long-range forces between charged objects but cannot replace the full numerical resolution of the PB equation at shorter separations.

Before closing this section, we recall the formal analogies and differences between the approach based on the bulk OZ equation with MSA–HNC closures and the approach based on the PB equation. To identify both theories, one must first neglect the ionic size and use the MSA for the ion–ion correlations in the OZ approach. Then, in the case of one isolated colloid immersed in an electrolyte ($\rho_c = 0$), the PB (DH) ionic profiles, $\rho_i(r)$, are rigorously identical to those obtained with the HNC (MSA) colloid–ion closure, $\rho_i' g_{ci}(r)$. In the presence of many colloids, this equivalence remains valid if the ensemble of particles is formally considered as constituting one single object of complex geometry immersed at infinite dilution in the supporting electrolyte. In that case, the colloid–ion functions lose the spherical symmetry and the integral equation requires a non-trivial numerical treatment which could serve as an alternative to the standard PB resolution [102]. On the other hand, the conventional OZ approach described in 4.2, although formally exact, is more sensitive to the neglect of the bridge functions. For example, at infinite dilution in colloids, the potential of mean force is given by

$$\beta W_{cc} = -\ln(g_{cc}) = \beta v_{cc} - \sum_{ion} \rho_i h_{ci} \otimes c_{ic} - b_{cc} \tag{69}$$

where the functions h_{ci} and c_{ci} represent the correlations of the ions with one isolated particle. So far, no approximation is made. Neglecting the bridge function b_{cc} implies that the force between two colloids is related to the one-body ionic profiles. This is clearly equivalent to a weak-overlap approximation, valid only at large separations. In that asymptotic regime, PB (DH) and HNC (MSA) forces coincide. At shorter distances, the conventional HNC–MSA theory misses the non-additive overlap corrections implicitly contained in b_{cc}. This explains in particular why the screened coulombic DLVO potential (56) is valid at all separations, *up to* contact, using the OZ–MSA route and at large separations only using the PB–DH route.

From the thermodynamics point of view, the analogy between both approaches subsists. Taking the linearized version of the PB equation (62), neglecting for simplicity the colloidal size and inserting the linear superposition of one-body electrostatic potentials (66) in the virial expression (65) makes it possible to recover almost completely the osmotic pressure (50). The single difference is the disappearance of the $-\kappa^3/24\pi$ term which obviously results from the neglect of the ion–ion correlation function $h_{ss}(r, r')$ [20] (zero-body term in the potential of mean force (15)).

4.4. Beyond DLVO—effective attraction between colloids

The existence of an effective attraction of pure electrostatic origin between like-charged particles via their counter-ions is a fascinating phenomenon which was predicted by Oosawa in the 1960s [103] and intensively studied in various geometry since the early 1980s. Many controversies in the literature have accompanied its description. As said in the introduction, the reason is certainly the intrinsic complexity of highly charged, asymmetrical mixtures and the difficulty of controlling the validity of approximations more or less implicitly assumed in theories in the absence of exact simulation data. It is clear that such attraction could be predicted only beyond the mean-field PB–DH–MSA–DLVO picture by including in some way ion–ion correlation effects. The studies which seem to invalidate this assertion by exhibiting attraction within a mean-field treatment are not satisfying. Without being exhaustive, the Sogami–Ise attraction derived within the DH approximation [104] (the form of this attraction is similar to (49)) has been proven to be due to an incorrect thermodynamical treatment [20, 105]. Equivalently, the claim for a non-DLVO attraction from the PM–MSA solution results from a confusion between mean-force and effective potentials [76]. In confined geometry, we recall that the general PB proof of pure repulsion between two colloids [96] *a posteriori* and definitely invalidates the attraction PB predictions, which may be due to insufficiently precise numerical resolutions [97] or to approximations used outside their domain of validity in analytical resolutions [101].

The situation is perfectly clear in the simple planar geometry of two identical, parallel, homogeneously charged plates separated by a continuous solvent containing the counter-ions and salt ions. As early as 1984, both Monte Carlo simulations [106] and inhomogeneous HNC calculations [107] within the PM have proven without ambiguity the existence of attraction between the plates (negative pressure) at high electrostatic coupling, e.g. at high surface charge density, ionic valence or Bjerrum length. The attraction appears when the two condensation shells strongly overlap at short separation resulting in non-obvious ion–ion correlations [108] and non-monotonic ionic profiles [109]. Although it exists in principle for all valences, it takes place in practice, for realistic charged plates in water, only in the presence of divalent or more highly charged counter-ions. Since the pioneer works, the phenomenon of attraction has been reproduced and analysed by numerous studies using different non-mean-field theories like the partially inhomogeneous three-point extension integral equation [110], the DFT with correlation contributions in the WDA version [111], the conventional homogeneous HNC integral equation with addition of the first bridge diagram [112], the MC simulation on a hypersphere [113], ... The attraction may be enhanced by the adsorption of additional chemical counter-ion adsorption and/or by surface charge heterogeneity ('long-range hydrophobic' attraction) [114]. In that last picture, the plates are considered as two-dimensional electrolytes or ionic crystals which spontaneously adjust complementary to each other. From the experimental point of view, attractive forces between charged plates immersed in aqueous calcium solutions have been directly measured with SFA and AFM techniques [115] and monitor the behaviour of clay suspensions and cements.

For bulk systems of spherical colloids, the situation is not so clear. Theoretical evidences of effective attraction have been first obtained following the integral equation approach. Using the bulk HNC closure for all pair correlations, Patey considered the case of two colloids immersed in an electrolyte and found attractive values in $w_{cc} \equiv v_{cc}^{eff}$ [116]. The same full HNC equation reveals at finite colloidal density and high electrostatic coupling an instability of the PM with respect to liquid–gas transition [80, 117]. As the colloidal or ionic charge is increased, the osmotic compressibility and $S_{cc}(0)$ take higher and higher values and seem to diverge (for the precise nature of the boundary line, see [118]). At the same time, the
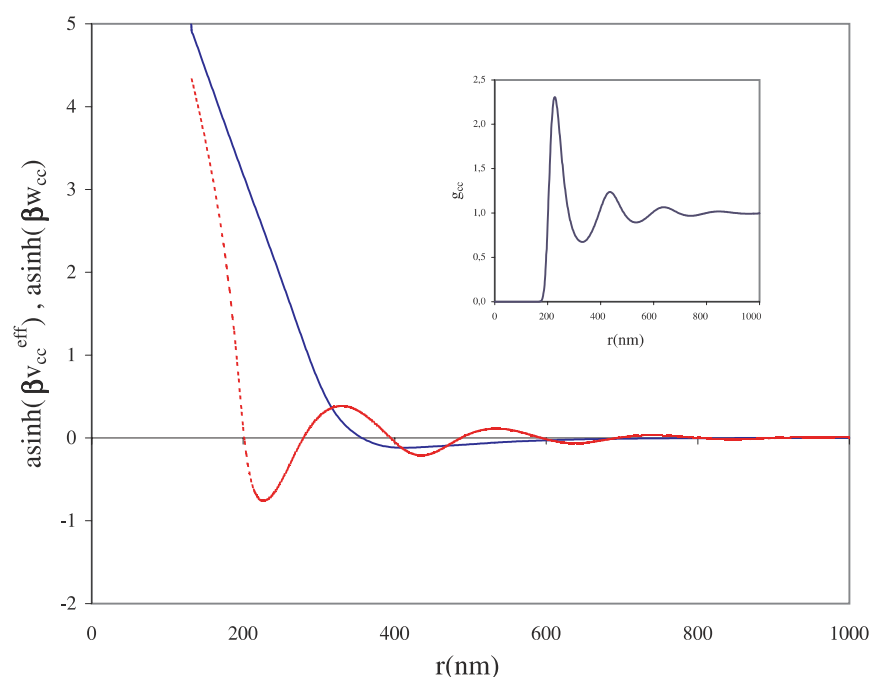
Figure 5. Effective $v_{cc}^{eff}(r)$ (solid line) and mean force $w_{cc}(r)$ (dotted line) pair potentials between colloids in salt-free, colloid + counter-ion primitive model. $T = 298$ K, $\varepsilon = 78$, $\sigma_i = 100$ nm/0, $Z_i = +300/-1$, $\Phi_c = 5\%$. Note the $a$sinh scale on the vertical axis. Inset: corresponding pair distribution function $g_{cc}(r)$. HNC integral equations in the PM and effective OCM.

free energy or virial routes do not present such instability, revealing a HNC thermodynamic inconsistency, the inverse of the DH–MSA one [80]. The location of the two-phase region and of the critical point in the density–temperature phase diagram depends on the charge asymmetry and on the colloid–counter-ion contact distance σ_{ci} [117]. Addition of salt tends to stabilize the system and shifts the critical point towards lower temperature [28]. As expected from the general analysis in sections 2.4 and 4.2, the state-dependent, OCM, effective potential v_{cc}^{eff} shifts from pure repulsion to partial attraction as the two-phase region is approached [28]. An example is given in figure 5 for a typical salt-free colloidal system $\sigma_i = 0/100$ nm, $Z_i = +300/-1$. The attraction is enhanced in the presence of ionic adsorption onto the colloids (charge regulation) [119]. To what extent could this behaviour be due to a failure of the HNC equation? Numerous tests indicate that the phase transition is an intrinsic property of the PM itself and that the quantitative HNC weakness is to overestimate the attraction and to predict the transition too soon, at too low coupling. The planar geometry limit as well as the restricted PM version (RPM) of symmetrical electrolytes [75, 118] constitute two extreme cases which illustrate this general trend. In between, Patey's attraction disappears for monovalent ions but subsists for divalent ions when including the first bridge diagram [112]. The bulk two-phase region is shifted towards higher charges [120] when the HNC closure is replaced by the thermodynamically consistent ZH closure [121].

Simulation data are obviously necessary to quantify the strength of the attraction and to determine the precise location of the critical point in the phase diagram. Since the early 1980s, the few MC and MD simulations performed in the micellar regime ($\sigma_c = 2$–3 nm, $Z_c = 10$–20) with monovalent counter-ions [65–67] show a short-range liquid order among the colloids
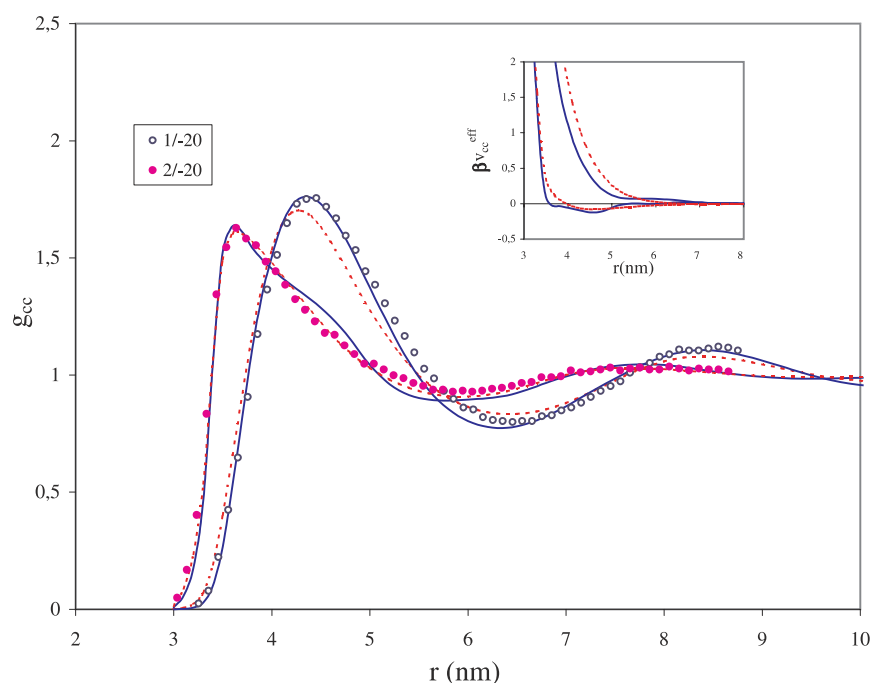
Figure 6. Colloid–colloid pair distribution function $g_{cc}(r)$ in salt-free, colloid + counter-ion primitive model. $T = 298$ K, $\varepsilon = 78.4$, $\sigma_i = 3$ nm/0.4 nm, $Z_i = +20/-1$ or -2, $\rho_c = 0.02$ M ($\Phi_c = 17\%$). MC data [69] (symbols), HNC (dotted lines) and BHP (solid lines) integral equation. Inset: corresponding effective colloid–colloid pair potentials $v_{cc}^{eff}(r)$ extracted using the same HNC and BHP integral equations in the effective OCM.

which is consistent with a purely repulsive effective potential, although no v_{cc}^{eff} has been directly extracted from the simulated g_{cc} in practice. HNC [65–67] and advanced closures [122] have been tested against these exact data (anecdotally, the first MC case published in the literature [65] was located inside the HNC two-phase region). More recent MC works have shown how this DLVO-like picture breaks down in the presence of *divalent* counter-ions [69]. Figure 6 presents MC $g_{cc}(r)$ for $+20/-1$ and $+20/-2$ systems at the same colloid volume fraction (5%) [69]. In the former case, the data present a classical order peak located near the mean separation distance between macro-ions, while in the latter case the peak is shifted near contact and seems to reveal a short-range effective attraction. The same behaviour is predicted by the HNC integral equation. A good quantitative fit of the MC data is obtained for both valences using the powerful BHP integral equation [123], as shown in figure 6 [124]. This accurate closure evaluates advanced bridge functions from approximated three-body direct correlation functions. In order to get a definite and quantitative answer about the existence of effective attraction, it is necessary to extract the OCM potential v_{cc}^{eff} from the cc correlations. This is hardly possible from the simulation data due to the statistical noise and to the limited r range, which prevent precise Fourier transformations but can be done easily from the theory curves. The effective potentials v_{cc}^{eff} are plotted in figure 6. Considering the very good agreement between MC and theory in $g_{cc}(r)$, these potential curves should be close to the exact one. As expected, v_{cc}^{eff} remains repulsive at all distances for monovalent ions and presents a clear negative minimum at intermediate distances in the presence of divalent counter-ions. This confirms the pioneer HNC predictions and demonstrates without ambiguity that, on average,

the spherical macro-ions attract each other through the counter-ions in highly charged bulk solutions. The existence of a phase separation which could result from such attractions has received partial confirmation in very recent powerful simulations [71]. Trivalent ions induce the formation of large clusters containing many macro-ions inside the simulation box. The observed heterogeneity is consistent with a condensation phenomenon or a liquid–gas phase separation, analogous to that observed within the RPM. The complete structure of the PM phase diagram and, in particular, the competition of condensation with crystallization, again of pure electrostatic origin, remains to be elucidated.

An alternative to the difficult, time-consuming simulations in bulk is offered by the cell approach where only one or two spherical macro-ions are considered in a box. In the original case of one colloid located at the centre of the Wigner–Seitz spherical cell, MC data show a non-PB behaviour at high coupling [87]. As the colloidal charge Z_c is increased in the absence of salt, the counter-ion concentration at the cell edge (and thus the osmotic pressure or the effective charge) first increases, goes through a maximum and then decreases (MC or DFT–WDA) [125], in contradiction with the saturation effect predicted by the PB approximation [89]. This kind of instability indirectly announces the existence of attraction between highly charged particles. Recent simulations have investigated the situation of two colloids inside the same cell and derived pair potentials/forces as a function of the separation D [126–128]. As usual in such geometry, the role of the cell boundary must be controlled with caution in order to avoid undesirable effects. In presence of added salt, it is sufficient in principle to investigate large enough cells, $R \gg \kappa'^{-1}$, D. In practice, for obvious reasons of computer limitations, $\kappa' R$ is not very large and comparisons with simulations performed with periodic image condition are necessary to interpret the data with confidence [128]. In any case, such simulations solve exactly (at last!) the original DLVO problem of two isolated spherical colloids immersed in an infinite electrolyte. The force remains repulsive for monovalent ions and becomes attractive for divalent counter-ions [128]. On the other hand, interpretation of the MC results in salt-free situations ($\kappa' = 0$) [126, 127] is less obvious. The short-range attraction observed at high coulombic coupling (divalent ions in solvent of low dielectric constant) [127] seems to be more related to the potential of mean force w_{cc} rather than to the effective potential v_{cc}^{eff}. Indeed, the measured force is partly due to colloidal neighbours which are hidden outside the cell boundary. As said before, the colloidal density through the cell dimension is never an irrelevant factor in salt-free systems. Even if the entropy of ions associated with the very large cell volume wins over the colloid–ion attraction only at high dilution (logarithmic dependence of S on ρ_c) [89], correct sampling of the very few MC configurations with ions located near the cell edge should be monitored during the simulation. Anyway, the present cell approach with a fine control of boundary effects seems to be a promising simulation tool to derive information on ion-mediated colloidal interactions, cheaper and complementary to the PM bulk approach.

Experimental evidence of ion-mediated effective attraction between *spherical* colloids is still an open and controversial issue. While the DLVO picture including a pure, screened coulombic repulsion between colloids has successfully explained most of the observed behaviours for half a century, some particular phenomena have resisted such interpretation. Electrostatic colloid crystals obtained at low concentration in highly deionized conditions (monovalent counter-ions) have been studied by Ise *et al* by direct visualization using confocal laser scanning microscopy and by ultrasmall-angle x-ray scattering [51]. Both techniques reveal the presence of apparently empty regions or *voids* inside the crystal. This has been claimed to be evidence for a long-range attraction [104]. A more recent DFT analysis imputes the local demixion to the presence of the $-\kappa^3$ constant term in the DH-like virial equation of state (51) [100]. This experimental observation has not been reproduced by similar studies of highly deionized latex systems [5] and contradicts the direct force measurements between

isolated particles [14]. As said in section 3.2, a possible explanation of the disagreement could be the undesirable presence of charged polymer impurities released by the latex surfaces in some solutions which would induce a depletion attraction of electrostatic origin between colloids. In that mechanism, the voids would be full of undetectable polymers. In the same way, the macroscopic liquid–gas-like phase separation experimentally observed at low ionic strength [129] has been reanalysed in terms of ionic impurities [130].

These particular and controversial cases apart, there is no clear experimental confirmation of the PM effective attraction between spherical macro-ions. This should be opposed to the situation observed in other geometry as for parallel plates [115], parallel cylinders [131] or in flexible polyelectrolytes [132] where attraction has been more or less directly measured in various systems. The fact that the calculated and observed attraction is always coupled with the presence of multivalent counter-ions is the key point which should incite the experimentalists to replace the usual monovalent ions by divalent or trivalent ones in spherical colloidal systems. Chemical destabilization seems to be the limiting factor in practice.

5. Van der Waals and miscellaneous interactions

So far the interior of the colloids has been considered as an inert, structureless material. In reality, colloids are made of polar and polarizable molecules. Atoms themselves carry instantaneous, fluctuating electronic dipoles. Interactions between all permanent and induced dipoles belonging to the different colloids, averaged over the degrees of freedom of the polar solvent, define the so-called van der Waals (VW) or dispersion forces [133, 134]. This universal interaction due to correlations in polarization fluctuations is essentially attractive and tends to destabilize colloidal suspensions towards irreversible coagulation. Its theoretical description can be viewed as the ultimate task in the field of colloidal interactions due to its complexity (the present VW section has been paradoxically rejected to the end of the review for this reason). Indeed, a complete theory must involve electrodynamics, quantum mechanics and statistical mechanics and faces the fundamental problem of non-pair-wise additivity of the total interactions between all atoms/molecules/particles intrinsically associated with the presence of polarizability. The case of an isolated pair of atoms was solved by London in 1930. Then, summing all r^{-6} atom–atom pair interactions, Hamaker deduced simple forms for the pair potential between colloidal bodies, which are widely used in the literature [9]. The Hamaker constant, which characterizes the strength of the interaction, depends on the frequency-dependent polarizability $\alpha_i(\omega)$ of the colloid and solvent materials. In order to go beyond this pair-wise additivity approximation, valid in principle at low $\alpha_c - \alpha_s$ only, one must account for the multiple 'reflexions' of the electromagnetic waves between the different local, oscillating dipoles. In the microscopic description, this would require us to consider colloids as collections of fixed polarizable elementary volumes and solvent molecules as moving dipolar, polarizable particles and to statistically average the multi-body interactions over the dipole fluctuations and solvent spatial configurations. This is a formidable task even within classical mechanics and electrostatics. An alternative, macroscopic approach, proposed by Lifshitz in 1956, views colloids and solvent as *continuous* dielectric media, characterized by their dielectric response function $\varepsilon_i(\omega)$ [133, 134]. Solving the Maxwell equations for the electromagnetic fields and using quantum field theory makes it possible to derive the interaction between two dielectric bodies immersed in a third medium (note the parallelism with the scattering problem which involves the same concepts: in the microscopic Rayleigh–Gans theory, the intensity scattered by a colloid is decomposed as a sum of contributions due to all its atoms, taken as isolated; the macroscopic Mie theory accounts for multiple scattering inside the same colloid by solving the Maxwell equations in continuous media). In practice, this can be done in simple cases only,

essentially in the planar geometry. The Hamaker constant in the formal Hamaker expression is a complex function of the $\varepsilon_i(\omega)$ and can be calculated in principle from the experimental absorption or dispersion spectra on the whole frequency domain [133].

From this introduction, it is clear that the classical DLVO decomposition of the total colloidal interaction in sum of bare VW and extra (screened coulombic, hydration...) independent contributions, though useful, may appear somewhat artificial and inconsistent. All interactions are of long-range coulombic nature and thus must be coupled, revealing *miscellaneous* interactions. (i) The hydration and hydrophobic forces (section 3) due to the discrete solvent structure and to specific colloid–solvent affinity can be considered as a part of the VW force at short separation. The solvent layer near the colloidal surface may be affected by surface–solvent dipole–dipole VW coupling. Inversely, solvent depletion or adsorption should alter the local dielectric constant in the London–Lifshitz theory. (ii) In the presence of uniform or heterogeneous charges on the colloids and ions in the solvent, VW dipole fluctuations and PM charge correlations become coupled. Thus, dispersion interactions and electrostatic images due to dielectric discontinuities must be treated self-consistently. Ninham and Parsegian generalized the Lifshitz theory by including charge fluctuations in the electrolyte at the DH level [135]. The main result is that the static, 'zero-frequency' dispersion attraction becomes screened as $\exp(-2\kappa r)$. Advanced studies have been performed essentially in the planar geometry [114, 136] with a few exceptions for spheres [119, 137]. (iii) Lastly, the ion binding or physisorption to the colloidal surfaces, which drives a colloid–colloid enhanced attraction as seen before, may be induced by dispersion interactions acting on ions themselves. This could explain in a rational way [138] ion specific, non-generic effects like the lyotropic or Hofmeister series for coagulation/crystallization efficiency, the salting in/salting out phenomenon and the long-range hydrophobic attraction [139], experimentally observed for decades in protein or polyelectrolyte systems and not yet fully understood. The self-consistent description of all these *miscellaneous* interactions in bulk solutions of spherical colloids forms a challenge for theoreticians in the near future.

Acknowledgments

References

[1] Hansen J P and McDonald I R 1986 *Theory of Simple Liquids* (London: Academic)
[2] Lindner P and Zemb Th (ed) 1991 *Neutron, X-ray and Light Scattering: Introduction to an Investigative Tool for Colloidal and Polymeric Systems* (Amsterdam: North Holland)
[3] Corti M and Degiorgio V 1981 *J. Phys. Chem.* **85** 711
    Hayter J B and Penfold J 1981 *J. Chem. Soc. Faraday Trans.* I **77** 1851
    Chen S H 1986 *Annu. Rev. Phys. Chem.* **37** 351
[4] Parsegian V A, Rand R P, Fuller N L and Rau D C 1986 *Methods in Enzymology: Biomembranes, Protons and Water, Structure and Translocation* vol 127, ed L Packer (New York: Academic) p 400
    Véretout F, Delaye M and Tardieu A 1989 *J. Mol. Biol.* **205** 713
    Goodwin J W, Ottewill R H and Parentich A 1990 *Colloid Polym. Sci.* **268** 1131
    Dubois M, Zemb Th, Fuller N, Rand R P and Parsegian V A 1998 *J. Chem. Phys.* **108** 7855
[5] Reus V, Belloni L, Zemb Th, Lutterbach N and Versmold H 1997 *J. Physique II* **7** 603
[6] Bonnet-Gonnet C, Belloni L and Cabane B 1994 *Langmuir* **10** 4012
[7] Perrin J 1910 *J. Physique* **9** 5
    Piazza R, Bellini T and Degiorgio V 1993 *Phys. Rev. Lett.* **71** 4267
    Rutgers M A, Dunsmuir J H, Xue J Z, Russel W B and Chaikin P M 1996 *Phys. Rev.* B **53** 5043

[8] Sonneville-Aubrun O, Bergeron V, Gulik-Krzywicki T, Jönsson B, Wennerström H, Lindner P and Cabane B 2000 *Langmuir* **16** 1566
[9] Israelachvili J N 1991 *Intermolecular and Surface Forces* (San Diego: Academic)
[10] Ducker W A, Senden T J and Pashley R M 1991 *Nature* **353** 239
[11] Leal Calderon F, Stora T, Mondain Monval O, Poulin P and Bibette J 1994 *Phys. Rev. Lett.* **72** 2959
[12] Prieve D C, Luo F and Lanni F 1987 *Discuss. Faraday Chem. Soc.* **83** 297
     Prieve D C and Walz J Y 1993 *Appl. Opt.* **32** 1629
     Flicker S G and Bike S G 1993 *Langmuir* **9** 257
[13] Vondermassen K, Bongers J, Mueller A and Versmold H 1994 *Langmuir* **10** 1351
[14] Crocker J C and Grier D G 1994 *Phys. Rev. Lett.* **73** 352
[15] Kepler G M and Fraden S 1994 *Phys. Rev. Lett.* **73** 356
[16] Crocker J C and Grier D G 1996 *Phys. Rev. Lett.* **77** 1897
[17] McMillan W G Jr and Mayer J E 1945 *J. Chem. Phys.* **13** 276
[18] Kirkwood J G and Buff F P 1951 *J. Chem. Phys.* **19** 774
[19] Friedman H L and Dale W D T 1977 *Modern Theoretical Chemistry* **5** ed B J Berne (New York: Plenum) ch 3
[20] Beresford-Smith B, Chan D Y and Mitchell D J 1984 *J. Colloid Interface Sci.* **105** 216
[21] Lekkerkerker H N W, Poon W C K, Pusey P N, Stroobants A and Warren P B 1992 *Europhys. Lett.* **20** 559
     Lekkerkerker H N W, Buining P, Buitenhuis J, Vroege G J and Stroobants A 1995 *Observation, Prediction and Simulation of Phase Transitions in Complex Fluids* ed M Baus *et al* (Dordrecht: Kluwer) 53
[22] Fushiki M 1992 *J. Chem. Phys.* **97** 6700
[23] Dijkstra M, van Roij R and Evans R 1999 *Phys. Rev.* E **59** 5744
[24] One simple rigorous way to derive this expression is to define the potential of mean force from the N_c-body colloid distribution function and take the limit of zero colloidal activity in the full grand canonical ensemble.
[25] Adelman S A 1976 *J. Chem. Phys.* **64** 724
[26] Beresford-Smith B and Chan D Y C 1982 *Chem. Phys. Lett.* **92** 474
     Senatore G and Blum L 1985 *J. Phys. Chem.* **89** 2676
[27] Belloni L 1986 *J. Chem. Phys.* **85** 519
[28] Belloni L 1987 *Thèse d'Etat* Paris VI
[29] Khan S, Morton T L and Ronis D 1987 *Phys. Rev.* A **35** 4295
[30] Henderson R L 1974 *Phys. Lett.* A **49** 197
[31] Asakura S and Oosawa F 1954 *J. Chem. Phys.* **22** 1255
[32] Poon W C K and Pusey P N 1995 *Observation, Prediction and Simulation of Phase Transitions in Complex Fluids* ed M Baus *et al* (Dordrecht: Kluwer) p 3
[33] Attard P 1989 *J. Chem. Phys.* **91** 3083
[34] Vrij A 1976 *Pure Appl. Chem.* **48** 471
[35] Biben T and Hansen J P 1991 *Phys. Rev. Lett.* **66** 2215
[36] Gast A P, Hall C K and Russel W B 1983 *J. Colloid Interface Sci.* **96** 251
[37] Walz J Y and Sharma A 1994 *J. Colloid Interface Sci.* **168** 485
[38] Mao Y, Cates M E and Lekkerkerker H N W 1995 *Physica* A **222** 10
[39] Christenson H K and Horn R G 1985 *Chem. Scr.* **25** 37
[40] Rudhardt D, Bechinger C and Leiderer P 1998 *Phys. Rev. Lett.* **81** 1330
[41] Sanyal S, Easwar N, Ramaswamy S and Sood A K 1992 *Europhys. Lett.* **18** 107
[42] Louis A A, Finken R and Hansen J P 2000 *Phys. Rev.* E **61** R1028
[43] Forsman J, Woodward C E and Jönsson B 1997 *J. Colloid Interface Sci.* **195** 264
[44] Claesson P M, Kjellander R, Stenius P and Christenson H K 1986 *J. Chem. Soc. Faraday Trans. I* **82** 2735
[45] Bibette J, Roux D and Nallet F 1990 *Phys. Rev. Lett.* **65** 2470
[46] Richetti P and Kékicheff P 1992 *Phys. Rev. Lett.* **68** 1951
[47] Sharma A and Walz J Y 1996 *J. Chem. Soc. Faraday Trans.* **92** 4997
     Sharma A, Tan S N and Walz J Y 1997 *J. Colloid Interface Sci.* **191** 236
[48] Hanley H J M, Straty G C and Lindner P 1994 *Langmuir* **10** 72
     Ottewill R, Hanley H J M, Rennie A R and Straty G C 1995 *Langmuir* **11** 3757
[49] Lutterbach N, Versmold H, Reus V, Belloni L, Zemb Th and Lindner P 1999 *Langmuir* **15** 345
[50] Spalla O personal communication
[51] Dosho S *et al* 1993 *Langmuir* **9** 394
     Ise N, Konishi T and Tata B V R 1999 *Langmuir* **15** 4176
[52] Attard P, Ursenbach C P and Patey G N 1992 *Phys. Rev.* A **45** 7621
[53] Napper D H 1983 *Polymeric Stabilisation of Colloidal Dispersions* (London: Academic)
[54] Lafuma F, Wong K and Cabane B 1991 *J. Colloid Interface. Sci.* **123** 9
[55] Spalla O, Nabavi M, Minter J and Cabane B 1996 *Colloid. Polym. Sci.* **274** 555

[56] Peyre V, Spalla O, Belloni L and Nabavi M 1997 *J. Colloid Interface Sci.* **187** 184
[57] Israelachvili J and Wennerström H 1996 *Nature* **379** 219
[58] Parsegian V A, Rand R P and Fuller N L 1991 *J. Phys. Chem.* **95** 4777
Ricoul F, Dubois M, Belloni L and Zemb Th 1998 *Langmuir* **14** 2645
[59] Kusalik P G and Patey G N 1988 *Mol. Phys.* **65** 1105
Torrie G M, Kusalik P G and Patey G N 1988 *J. Chem. Phys.* **88** 7826
Attard P, Wei D, Patey G N and Torrie G M 1990 *J. Chem. Phys.* **93** 7360
[60] Forsman J, Woodward C E and Jönsson B 1997 *Langmuir* **13** 5459
[61] Weeks J D, Katsov K and Vollmayr K 1998 *Phys. Rev. Lett.* **81** 4400
Lum K, Chandler D and Weeks J D 1999 *J. Phys. Chem.* B **103** 4570
[62] Marcelja S 1997 *Colloid Surf. A* **129/130** 321
[63] Marcelja S 1997 *Nature* **385** 689
Israelachvili J N and Wennerström H 1997 *Nature* **385** 689
[64] Verwey E J W and Overbeek J Th G 1948 *Theory of Stability of Lyophobic Colloids* (Amsterdam: Elsevier)
[65] Linse P and Jönsson 1982 *J. Chem. Phys.* **78** 3167
[66] Vlachy V, Marshall C H and Haymet A D J 1989 *J. Am. Chem. Soc.* **111** 4160
[67] Linse P 1990 *J. Chem. Phys.* **93** 1376
[68] Delville A 1994 *Langmuir* **10** 395
[69] Hribar B, Kalyuzhnyi Y V and Vlachy V 1996 *Mol. Phys.* **87** 1317
Hribar B and Vlachy V 1997 *J. Phys. Chem.* B **101** 3457
Lobaskin V and Linse P 1998 *J. Chem. Phys.* **109** 3530
[70] Lobaskin V and Linse P 1999 *J. Chem. Phys.* **111** 4300
[71] Linse P and Lobaskin V 1999 *Phys. Rev. Lett.* **83** 4208
Hribar B and Vlachy V 2000 *Biophys. J.* **78** 694
[72] Torrie G M and Valleau J P 1980 *J. Chem. Phys.* **73** 5807
Jönsson B, Wennerström H and Halle B 1990 *J. Phys. Chem.* **84** 2179
Megen W and Snook I 1980 *J. Chem. Phys.* **73** 4656
[73] Langmuir 1938 *J. Chem. Phys.* **6** 873
[74] Levin Y and Fisher M E 1996 *Physica* A **225** 164
Zuckerman D M, Fisher M E and Lee B P 1997 *Phys. Rev.* E **56** 6569
[75] Orkoulas G and Panagiotopoulos A Z 1994 *J. Chem. Phys.* **101** 1452
Caillol J M, Levesque D and Weis J J 1996 *Phys. Rev. Lett.* **77** 4039
Orkoulas G and Panagiotopoulos A Z 1999 *J. Chem. Phys.* **110** 1581
[76] Chu X and Wasan D T 1996 *J. Colloid Interface. Sci.* **184** 268
[77] Warren P B 2000 *J. Chem. Phys.* **112** 4683
[78] Medina-Noyola M and McQuarrie D A 1980 *J. Chem. Phys.* **73** 6279
[79] Blum L and Hoye J S 1977 *J. Phys. Chem.* **81** 1311
[80] Belloni L 1985 *Chem. Phys.* **99** 43
[81] Hoskin N E and Levine S 1955 *Trans. R. Soc.* A **248** 433
Hoskin N E and Levine S 1955 *Trans. R. Soc.* A **248** 449
Bell G M and Levine S 1957 *Trans. Faraday Soc.* **53** 143
Bell G M and Levine S 1957 *Trans. Faraday Soc.* **54** 785
[82] Löwen H, Hansen J P and Madden P A 1993 *J. Chem. Phys.* **98** 3275
[83] Ninham B W and Parsegian V A 1971 *J. Theor. Biol.* **31** 405
[84] Evans R 1993 *Fundamentals of Inhomogeneous Fluids* ed D Henderson (New York: Dekker)
Hansen J P 1995 *Phase Transitions in Complex Fluids* ed M Baus, L F Rull and J P Ryckaert (Dordrecht: Kluwer)
[85] Houstis E N, Lynch R E, Rice J R and Papatheodorou T S 1978 *J. Comput. Phys.* **27** 323
Houstis E N, Mitchell W F and Papatheodorou T S 1985 *ACM Trans. Math. Software* **11** 379
Alvarez-Ramirez J, Martinez R and Diaz-Herrera E 1997 *Chem. Phys. Lett.* **266** 375
Warszynski P and Adamczyk 1997 *J. Colloid Interface Sci.* **187** 283
Bowen W R and Sharif A O 1997 *J. Colloid Interface Sci.* **187** 363
Tomac S and Gräslund A 1998 *J. Comput. Chem.* **19** 893
[86] Marcus R A 1955 *J. Chem. Phys.* **23** 1057
[87] Wennerström H, Jönsson B and Linse P 1982 *J. Chem. Phys.* **76** 4665
[88] Bell G M, Levine S and McCartney L N 1970 *J. Colloid Interface Sci.* **33** 335
[89] Oosawa F 1971 *Polyelectrolytes* (New York: Dekker)
Manning G S 1969 *J. Chem. Phys.* **51** 924
Alexander S, Chaikin P M, Grant P, Morales G J, Pincus P and Hone D 1984 *J. Chem. Phys.* **80** 5776

Ramanathan C V 1988 *J. Chem. Phys.* **88** 3887
Kjellander R and Mitchell D J 1994 *J. Chem. Phys.* **101** 603

[90]   Belloni L 1998 *Colloid Surf.* A **140** 227

[91]   Again, the presence of the electrolyte ($\kappa' \neq 0$) is essential in this situation. If not, the counter-ions which equilibrate the charge of the two particles would leave the vicinity of the surfaces and occupy the infinite volume, whatever the strength of the electrostatic attraction (in other words, the entropy always wins over the energy at infinite dilution), and the force felt by the colloids would be the trivial, coulombic one.

[92]   Marcelja S, Mitchell D J, Ninham B W and Sculey M J 1977 *J. Chem. Soc. Faraday Trans. II* **73** 630
Glendinning A B and Russel W B 1983 *J. Colloid Interface Sci.* **93** 95
Carnie S L and Chan D Y C 1993 *J. Colloid Interface Sci.* **155** 297

[93]   Hoskin N E 1955 *Phil. Trans.* A **248** 433
Ledbetter J E, Croxton T L and McQuarrie D A 1981 *Can. J. Chem.* **59** 1860
Carnie S L, Chan D Y C and Stankovitch J 1994 *J. Colloid Interface Sci.* **165** 116

[94]   Robbins M, Kremer K and Grest G S 1988 *J. Chem. Phys.* **88** 3286

[95]   von Grünberg H H and Belloni L 2000 *Phys. Rev.* E **62** 2493

[96]   Neu J C 1999 *Phys. Rev. Lett.* **82** 1072
Sader J E and Chan D Y C 1999 *J. Colloid Interface Sci.* **203** 268

[97]   Bowen W R and Sharif A O 1998 *Nature* **393** 663

[98]   Carbajal-Tinoco M D, Castro-Roman F and Arauz-Lara J L 1996 *Phys. Rev.* E **53** 3745
Larsen A E and Grier D G 1997 *Nature* **385** 230

[99]   Hansen J P and Löwen H 2000 *Ann. Rev. Phys. Chem.* at press

[100] van Roij R, Dijkstra M and Hansen J P 1999 *Phys. Rev.* E **59** 2010

[101] Goulding D and Hansen J P 1999 *Europhys. Lett.* **46** 407

[102] Sanchez-Sanchez J E and Lozada-Cassou M 1992 *Chem. Phys. Lett.* **190** 202

[103] Oosawa F 1968 *Biopolymers* **6** 1633

[104] Sogami I 1983 *Phys. Lett.* A **96** 199
Sogami I and Ise N 1984 *J. Chem. Phys.* **81** 6320
Smalley M V 1990 *Mol. Phys.* **71** 1251
Sogami I S, Shinohara T and Smalley M V 1992 *Mol. Phys.* **76** 1

[105] Overbeek J Th G 1987 *J. Chem. Phys.* **87** 4406
Woodward C E 1988 *J. Chem. Phys.* **89** 5140
Overbeek J Th G 1993 *Mol. Phys.* **80** 685
Rosenfeld Y 1994 *Phys. Rev.* E **49** 4425
Jönsson B, Akesson T and Woodward C E 1996 *Ordering and Phase Transitions in Charged Colloids* ed A R Arora and B V R Tata (New York: VCH)

[106] Guldbrand L, Jönsson B, Wennerström H and Linse P 1984 *J. Chem. Phys.* **80** 2221
Valleau J P, Ivkov R and Torrie G M 1991 *J. Chem. Phys.* **95** 520

[107] Kjellander R and Marcelja S 1984 *Chem. Phys. Lett.* **112** 49
Kjellander R and Marcelja S 1985 *J. Chem. Phys.* **82** 2122
Kjellander R and Marcelja S 1986 *J. Chem. Phys.* **90** 1230

[108] Kjellander R 1996 *Ber. Bunsenges. Phys. Chem.* **100** 894

[109] Kjellander R, Akesson T, Jönsson B and Marcelja S 1992 *J. Chem. Phys.* **97** 1424

[110] Lozada-Cassou M 1984 *J. Chem. Phys.* **80** 3344
Lozada-Cassou M and Henderson D 1986 *Chem. Phys. Lett.* **127** 392
Lozada-Cassou and Diaz-Herrera E 1990 *J. Chem. Phys.* **92** 1194

[111] Stevens M J and Robbins M O 1990 *Europhys. Lett.* **12** 81
Tang Z, Scriven L E and Davis H T 1992 *J. Chem. Phys.* **97** 9258

[112] Attard P and Miklavic S J 1993 *J. Chem. Phys.* **99** 6078

[113] Delville A, Pellenq R J M and Caillol J M 1997 *J. Chem. Phys.* **106** 7275

[114] Attard P, Kjellander R, Mitchell D J and Jönsson B 1988 *J. Chem. Phys.* **89** 1664
Podgornik R 1989 *J. Chem. Phys.* **91** 5840
Miklavic S J, Chan D Y C, White L R and Healy T W 1994 *J. Phys. Chem.* **98** 9022
Rouzina I and Bloomfield V A 1996 *J. Phys. Chem.* **100** 9977
Forsman J, Jönsson B and Akesson T 1998 *J. Phys. Chem.* B **102** 5082

[115] Kékicheff P, Marcelja S, Senden T J and Shubin V E 1993 *J. Chem. Phys.* **99** 6098

[116] Patey G N 1980 *J. Chem. Phys.* **72** 5763

[117] Belloni L 1986 *Phys. Rev. Lett.* **57** 2026

[118] Belloni L 1993 *J. Chem. Phys.* **98** 8080

[119] Belloni L and Spalla O 1997 *J. Chem. Phys.* **107** 465
[120] Belloni L 1988 *J. Chem. Phys.* **88** 5143
[121] Zerah H and Hansen J P 1986 *J. Chem. Phys.* **84** 2336
[122] Rescic J, Vlachy V and Haymet A D J 1990 *J. Am. Chem. Soc.* **112** 3398
      Kalyuzhnyi Y V, Vlachy V, Holovko M F and Stell G 1995 *J. Chem. Phys.* **102** 5770
[123] Barrat J L, Hansen J P and Pastore G 1988 *Mol. Phys.* **63** 747
[124] Belloni L, to be published
[125] Groot R D 1991 *J. Chem. Phys.* **95** 9191
[126] D'Amico I and Löwen H 1997 *Physica* A **237** 25
      Allahyarov E, Löwen H and Trigger S 1998 *Phys. Rev.* E **57** 5818
[127] Allahyarov E, D'Amico I and Löwen H 1998 *Phys. Rev. Lett.* **81** 1334
[128] Wu J, Bratko D and Prausnitz J M 1998 *Proc. Natl Acad. Sci.* **95** 15 169
      Wu J Z, Bratko D, Blanch H W and Prausnitz J M 1999 *J. Chem. Phys.* **111** 7084
[129] Tata B V R, Rajalakshmi M and Arora A K 1992 *Phys. Rev. Lett.* **69** 3778
[130] Palberg T and Würth M 1994 *Phys. Rev. Lett.* **72** 786
[131] Bloomfield V A 1991 *Biopolymers* **31** 1471
      Leikin S, Parsegian V A, Rau D C and Rand R P 1993 *Annu. Rev. Phys. Chem.* **44** 369
      Sikorav J L, Pelta J and Livolant F 1994 *Biophys. J.* **67** 1
      Tang J X, Wong S, Tran P and Janmey P 1996 *Ber. Bunsenges. Phys. Chem.* **100** 1
[132] Olvera de la Cruz M, Belloni L, Delsanti M, Dalbiez J P, Spalla O and Drifford M 1995 *J. Chem. Phys.* **103** 5781
[133] Mahanty J and Ninham B W 1976 *Dispersion Forces* (New York: Academic)
[134] Hunter R J 1987 *Foundations of Colloid Science* vol 1 (Oxford: Clarendon) ch 4
[135] Ninham B W and Parsegian A V 1972 see chapter 7 of reference [133]
[136] Attard P, Kjellander R and Mitchell D J 1987 *Chem. Phys. Lett.* **139** 219
      Kjellander R and Marcelja S 1987 *Chem. Phys. Lett.* **142** 485
      Attard P, Mitchell D J and Ninham B W 1988 *J. Chem. Phys.* **89** 4358
[137] Levin Y 1999 *Physica* A **265** 432
[138] Ninham B W, Kurihara K and Vinogradova O I 1997 *Colloid Surf.* A **123** 7
      Ninham B W and Yaminsky V 1997 *Langmuir* **13** 2097
[139] Spalla O 2000 *Current Opinion Col. Interf. Sci.* **5** 5